UNIVERSITÀ DEGLI STUDI DI PADOVA

Dipartimento di Scienze Oncologiche e Chirurgiche

SCUOLA DI DOTTORATO DI RICERCA IN

ONCOLOGIA E ONCOLOGIA CHIRURGICA

XXIV ciclo

Notch3 signalling promotes tumour growth in colorectal cancer: implication for Notch target therapy

DIRETTORE DELLA SCUOLA: Chia.ma Prof.ssa Paola Zanovello

TUTOR: Dr. Indraccolo Stefano

DOTTORANDA: Serafin Valentina

Anno Accademico 2010-2011

Ai miei genitori,
e ai miei colleghi di vita e di lab

“Ogni avversità porta con sé il seme dell’opportunità”

INDEX

RIASSUNTO

E’ ormai noto da alcuni anni che un’aberrante attivazione della via di segnalazione di Notch gioca un ruolo critico nella patogenesi della leucemia linfoblastica acuta a cellule T (T-ALL) e di alcune neoplasie solide come il cancro del polmone, della mammella e dell’ovaio. Inoltre, una marcata attivazione del recettore Notch1 è stata osservata negli adenomi intestinali ed è correlata all’aumentata espressione del ligando Jagged-1 indotta dall’attivazione del *pathway* Wnt-APC-β-catenina.

E’ stato inoltre dimostrato che questa *pathway*, insieme a quella di Notch, interviene nella regolazione della proliferazione e del differenziamento delle cellule epiteliali della mucosa intestinale normale. Attualmente, non si sa ancora se altri meccanismi di attivazione della *pathway* di Notch, oltre a quello ligando-dipendente, siano operativi nel CRC e nemmeno se possano essere coinvolti altri recettori della stessa famiglia.

In questo studio, abbiamo cercato di chiarire il possibile coinvolgimento di Notch3 nel CRC. Basandoci sull’osservazione che Notch3 risulta essere frequentemente overespresso sia a livello di mRNA che di proteina nei campioni umani di CRC, abbiamo cercato di chiarire come il recettore Notch3 potesse modulare le proprietà tumorigeniche delle cellule di CRC. A tale scopo, si sono rivelati particolarmente utili alcuni xenotrapianti di cellule umane di CRC che presentano una diversa aggressività in topi NOD/SCID. Infatti, utilizzando i tumori sperimentali, abbiamo potuto dimostrare che l’espressione dei diversi componenti del *pathway* di Notch risulta essere significativamente elevata nella variante aggressiva rispetto a quella dormiente. In particolare si è osservata un’ aumentata espressione dei ligandi DLL4 e Jagged-1 ed un incremento dei livelli del trascritto di *Notch3* e della forma attiva del recettore nei tumori che crescono più rapidamente. Una simile up-regolazione di Notch3 con un’aumentata attivazione della via di segnalazione si è osservata in seguito a stimolazione delle cellule di CRC in *vitro* con il ligando DLL4 ricombinante.

Analogamente, anche l’overespressione di una forma attiva del recettore Notch3 in queste stesse cellule conferisce loro una maggiore capacità proliferativa e favorisce la formazione di tumori in *vivo*. Al contrario, si è visto che l’inattivazione

del *pathway* mediante silenziamento genico di Notch3 nelle cellule aggressive di CRC, determina significative alterazioni del ciclo cellulare con conseguente riduzione nella proliferazione *in vitro* e un ritardo nella crescita dei tumori *in vivo*.
Complessivamente, questi risultati dimostrano che il recettore Notch3 può modulare le proprietà tumorigeniche delle cellule di CRC, in particolare contribuendo a mantenere elevata l'attivazione della via di Notch nei tumori esprimenti nel loro microambiente tumorale alti livelli di DLL4.
Inoltre, l'inoculo della variante più aggressiva rispetto a quella dormiente per via endovenosa in topi NOD/SCID ha mostrato che le cellule di CRC non hanno solo una diversa capacità tumorigenica, ma anche una differente capacità metastatica a livello polmonare, sia in termine di numero che di dimensioni delle metastasi osservate.
Basandoci sui risultati fin qui ottenuti, e su uno studio recentemente pubblicato in cui è stato dimostrato come il *pathway* di Notch sembra essere coinvolto anche nel processo di metastatizzazione, abbiamo condotto un primo esperimento pilota che prevedeva, in topi portatori di metastasi polmonari, il blocco dei recettori Notch3 e Notch2 mediante l'impiego di un anticorpo neutralizzante.
Sfortunatamente i risultati ottenuti non hanno fino ad ora mostrato una riduzione significativa nel numero e nelle dimensioni delle metastasi analizzate: l'analisi dei livelli di alterazione di Notch dopo il trattamento è in corso.
A conclusione dello studio le nostre osservazioni rappresentano un punto di partenza per un futuro sviluppo di terapie che abbiano Notch3 come bersaglio per il trattamento di un sottogruppo di casi di CRC.

ABSTRACT

It is well known that aberrant activation of the Notch pathway plays a critical role in the pathogenesis of T cell acute lymphoblastic leukaemia (T-ALL) and of certain solid tumors including lung, breast and ovarian cancer. In particular, increased Notch1 activity has been observed in intestinal adenoma, partially accomplished by β-catenin-mediated up-regulation of the Notch ligand Jagged-1.

Whether further mechanisms of Notch activation exist and other Notch receptors might be involved in colorectal cancer (CRC) has not been investigated so far. In this study we investigated the possible involvement of Notch3 signaling in CRC, and the possible therapeutic implications.

Intrigued by the observation that Notch3 mRNA and protein are over-expressed in a subset (20%) of human CRC, we sought to investigate how Notch3 modulates oncogenic features of CRC cells. By exploiting xenografts of CRC cells with different tumorigenic properties in mice, we found that the aggressive phenotype was associated with altered expression of components of the Notch pathway, including augmented expression of Delta-like 4 (DLL4) and Jagged-1 ligands and increased levels of the Notch3 transcript and intracellular domain (ICD). Stimulation with immobilized recombinant DLL4 dramatically increased Notch3 expression and Notch signaling. Moreover, forced expression of an active form of Notch3 mirrored effects of DLL4 stimulation and increased tumor formation. Conversely, blocking Notch3 signaling resulted in perturbation of the cell cycle followed by reduction of cell proliferation and inhibition of tumor growth.

Moreover, we observed that these CRC cells have also different metastatic potential in terms of number and dimension when injected intravenously in mice.

Lung metastases formed by CRC cells expressed Notch3, but the number or size was not significantly reduced by anti-Notch2/3 treatment.

Overall, these findings indicate that Notch3 receptor can modulate the tumorigenic properties of CRC cells, and that DLL4 contributes to sustain Notch activity in DLL4-expressing tumors. Further studies are necessary to clarify the role of Notch3 in metastasis and design effective target therapies.

1. INTRODUCTION

1.1 Epidemiology of Colo-Rectal Carcinoma (CRC)

1.1.1 CRC carcinogenesis

In developed countries malignant tumors are the second most common cause of death, after cardiovascular diseases, comprising 23-25 percent of total mortality. Colo-rectal cancer is the third more frequent tumor both in men and women after prostate or breast cancer respectively, and lung cancer (1). The risk of developing colorectal cancer increases with age. Most cases occur in the 60s and 70s, while cases before age 50 are uncommon unless a family history of early colon cancer is present (2).

The etiological factors and pathogenetic mechanisms underlying CRC development appear to be complex and heterogeneous. Contributory agents and mechanisms in CRC include dietary and lifestyle factors as well as inherited mutations. Among the most significant risk factors for CRC appear to be a diet rich in unsaturated fats and red meat, total energy intake, excessive alcohol consumption, and reduced physical activity (3).

In contrast to the modest progress achieved in defining lifestyle and environmental risk factors, there has been significant progress in identifying the specific gene defects that underlie inherited predisposition to CRC, as well as the constellation of somatic (i.e., arising in nongerm cells during the patient's lifetime) alterations that are present in sporadic CRCs.

A present estimate is that 15–30% of CRCs may have a major **hereditary** component, given the occurrence of CRC in first- or second-degree relatives. The bulk of these highly penetrant cases are attributable to the hereditary nonpolyposis colorectal cancer (HNPCC) syndromes, and another significant subset is associated with familial adenomatous polyposis (FAP) and closely related variant syndromes.

I. **HNPCC** was one of the first inherited cancer syndromes to be described in depth in the medical literature, specifically in Warthin's description of a three-generation family with HNPCC. Many years later, Lynch *et al*. (4) highlighted kindreds with autosomal dominant patterns not accompanied by extensive polyposis, with an 80% life-time risk of CRC, and 50–60% life-time risk of endometrial cancer in women. Genetic studies clearly established that HNPCC was a genetically heterogeneous disease, caused by mutations in one of the mismatch repair genes, most commonly *hMLH1*, *hMSH2* and *hMSH6*. Loss of DNA mismatch repair function in HNPCC, therefore, requires both the germline mutation and a somatic hit, so that the cell loses its ability to correct errors during DNA replication. The most vulnerable areas to loss of mismatch repair mechanisms are poly-oligo tracts and base pair repeats known as microsatellites. Disruption of these sequences is seen in over 90% of CRCs arising in HNPCC patients, a phenomenon known as microsatellite instability (MSI). MSI is also seen in about 15% of sporadic CRC (5).

II. **FAP** is an autosomal dominant syndrome that accounts for ~0.5% of all CRCs. Hundreds to thousands of adenomas can arise in the colon and rectum of affected individuals by the third or fourth decade of life, although at most only a few adenomas progress to CRC in a given FAP patient. Because the lifetime incidence of CRC in untreated FAP patients approaches 100%, with a mean age of diagnosis of 36 years, prophylactic removal of the patient's colon early in adult life remains the mainstay of clinical management for FAP (6). Germ-line mutations in the *Adenomatous polyposis coli* (*APC*) tumor suppressor gene underlie FAP and FAP variant syndromes. Although a fraction of germ-line mutations in FAP patients cause *APC* gene–expression silencing, more than 95% of known mutations are frame-shift or nonsense mutations that lead to premature truncation of correspondent protein. Two hot spots at codons 1061 and 1309 account for nearly 35% of the mutations identified. Mutations between codons 1250 and 1464 are associated with particularly profuse forms of polyposis, whereas mutations that are N-terminal of codon 157 or near the C terminus lead to attenuated polyposis, a syndrome that in some cases is associated with as

few as 10 to 20 adenomas by 50 years of age (7). Since the APC protein has many well-characterized functional domains and interacts with numerous other proteins, its deregulation can perturb a wide variety of cellular processes including migration, adhesion, proliferation, and even perhaps aspects of chromosome stability and cytoskeletal organization. Indeed, regulation of cytoplasmic β-catenin levels requires appropriate complexing of APC, β-catenin, glycogen synthase kinase 3β (GSK3β) and axin. GSK3β is then able to phosphorylate β-catenin on specific serine and threonine residues, thus targeting it for ubiquitin-mediated degradation. In the absence of this regulation, β-catenin escapes degradation and translocates to the nucleus where it complexes with one of the T cell factor/lymphoid enhancer factor (TCF/LEF) and initiates transcription of a wide variety of genes. The downstream transcriptional activation targets of β-catenin include a number of genes involved in the development and progression of colorectal carcinoma, including cyclin D1 and the oncogene *c-myc*. Consistent with its definition as a tumor suppressor gene, bi-allelic disruption of the *APC* gene occurs in both FAP and sporadic CRCs (5).

A few other syndromes constitute the remainder of such highly penetrant cases (3).

Sporadic CRCs rappresent 70% of all cases that are diagnosed and they do not have a familiary story but the insurgence is due to dietary and lifestyle factors, microsatellite instability and somatic mutations. Genetic alterations found are of two types: mutations that lead to novel or increased function of oncogenes and loss of function of tumor-suppressor genes (TSGs). The conversion of cellular genes into oncogenic variant alleles can result from specific point mutations or rearrangements that alter gene structure and function or from chromosome rearrangements or amplifications that disrupt regulated gene expression. For example *KRAS* somatic mutations are found in approximately 40% of CRCs; the vast majority of *KRAS* mutations affect codon 12, a subset affect codon 13, and rare mutations affect codon 61. A small fraction of CRCs have *NRAS* mutations at codon 12, 13, or 61 (8). Moreover, approximately 90% of all sporadic CRCs have

constitutive activation of the β-catenin mediated transcriptional pathway, consequent on either *APC* or *CTNNB1* (β-catenin) mutations (5).

1.1.2 The multistep genetic models of CRC

The histological progression of colorectal cancer from adenoma to carcinoma was first described by *Morson* and colleagues and the genetic pathway which mediates this transition has been suggested by *Fearon, Vogelstein, Bodmer* and others.
In this model, that explains almost 85% of all CRC cases, dysplasia is usually taken as the first recognizable step in the adenoma-carcinoma sequence. Small areas of epithelium with irregular glandular architecture, termed aberrant crypt foci (ACF), have been reported to harbour mutations in *APC* and *KRAS* genes (Figure 1a). Moreover, p53 mutations occur more frequently in high-grade dysplastic polyps and are thought to mark the transition from adenoma to carcinoma (Figure 1a). Furthermore, the progression from adenomatous lesion to cancer is often in association with chromosomal instability (CIN) and *APC* inactivation has been suggested to play a role in CIN (3,5,8).

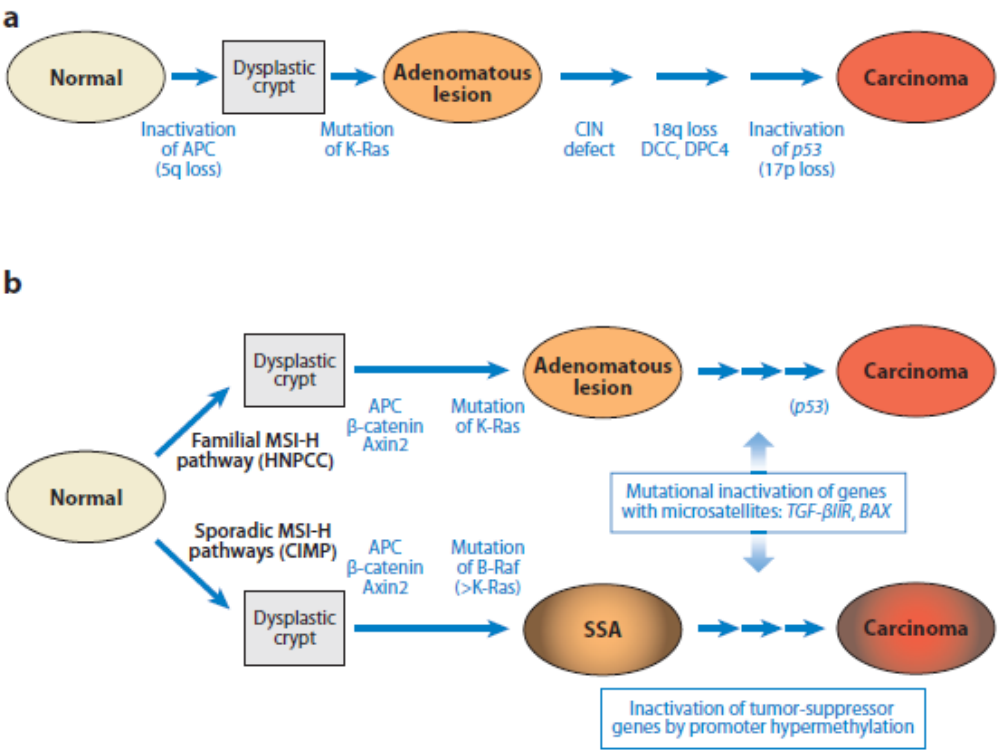

Figure 1: Genetic model of colorectal cancer (CRC). (a) Most CRCs are believed to arise from adenomatous polyps over a period of years or even decades. Selected inherited and somatic genetic alterations believed to underlie tumor initiation and progression are indicated. Although the order in which the gene defects arise is not invariant, the mutations show a strong association with particular stages of tumorigenesis. (b) In approximately 15% of CRCs, mismatch repair function is inactivated either by somatic mutations or by epigenetic inactivation, leading to high-frequency microsatellite instability. Subsequent alteration in the APC/β-catenin pathway together with mutations in K-Ras or B-Raf (in the case of sessile serrated adenomas (SSA)) proteins leads to adenoma formation. In the end in both familial and sporadic MSI-H tumors, inactivation of additional genes (e.g., *TGFβIIR*, *BAX*) might contribute to tumor progression (3,5).

However, from more recent studies there are evidences that in approximately 15% of CRCs defects in mismatch repair function are the major causes that drive colon cells to microsatellite instability (Figure 1b). Mismatch repair (MMR) function is inactivated either by somatic mutations or by epigenetic inactivation, leading to high-frequency microsatellite instability (MSI-H). Somatic mutational inactivation of MMR genes is most commonly observed as a second “hit” in patients who already carry germ-line mutations in MMR genes and whose tumors fall under the HNPCC

syndrome. Epigenetic inactivation of MMR genes most commonly affects hypermethylation of the *MLH1* promoter.
In the approximately 10–12% of apparently sporadic MSI-H CRCs, many of the cancers may arise as sessile serrated adenomas (SSAs), particularly those in the proximal colon, and some molecular lesions associated with the genesis of SSAs and their subsequent progression to CRC are distinct from those in the CIN- and HNPCC-type MSI-H CRCs. These molecular lesions include frequent *B-RAF* mutations and silencing of certain TSGs, which occurs in part via promoter hypermethylation and chromatin-remodeling events.
In both familial and sporadic MSI-H tumors, inactivation of genes (e.g., *TGFβIIR*, *BAX*) whose coding sequences contain repetitive elements (microsatellites) might contribute to tumor progression (3).

1.2 The Notch receptors family

The *Notch* gene was named for the phenotype of a mutant Drosophila with an indentation in the wings. In the 1930s, it was suggested that the genetic locus responsible for this phenotype has an important role in the cell fate decision during Drosophila embryogenesis and that the homozygous mutation of this locus results in excessive differentiation to neuronal tissue.
Only in the 1980s molecular cloning studies revealed that the *Notch* gene encodes a single-pass transmembrane protein that functions as a receptor for the ligand present on the cell surfaces of neighboring cells (9).
In mammals, a wide variety of cells use the Notch signaling system for embryonic development and, in adults, maintenance of tissue homeostasis. A number of studies have focused on the developmental biology, cell biology, and molecular biology of the Notch signaling cascade in individual cellular systems (10).

Human Notch genes are several and encode four different receptors. A prototypical Notch gene encodes a single transmembrane receptor composed in its extracellular region of a conserved array of up to 36 epidermal growth factor (EGF)-like repeats, involved in ligand interaction, followed by a cysteine-rich Notch

or LIN12 (LN) domain, a juxtamembrane region with specific proteinase cleavage sites, a transmembrane region including a cleavage site for γ-secretase, and a cytoplasmic region that contains several functional domains. Furthermore, the cytoplasmic region is composed by a RAM (RBP-Jκ- associated molecule) domain, a set of six ankyrin (ANK) repeats flanked by two nuclear localization sequences (NLSs), and by a transactivation (TAD) domain, which is present only in NOTCH1 and NOTCH2 but not in NOTCH3 or NOTCH4 receptor. Finally, the last domain (PEST) is composed by a tail of proline, glutamate, serine and threonine-rich sequence (11) (Figure 2).

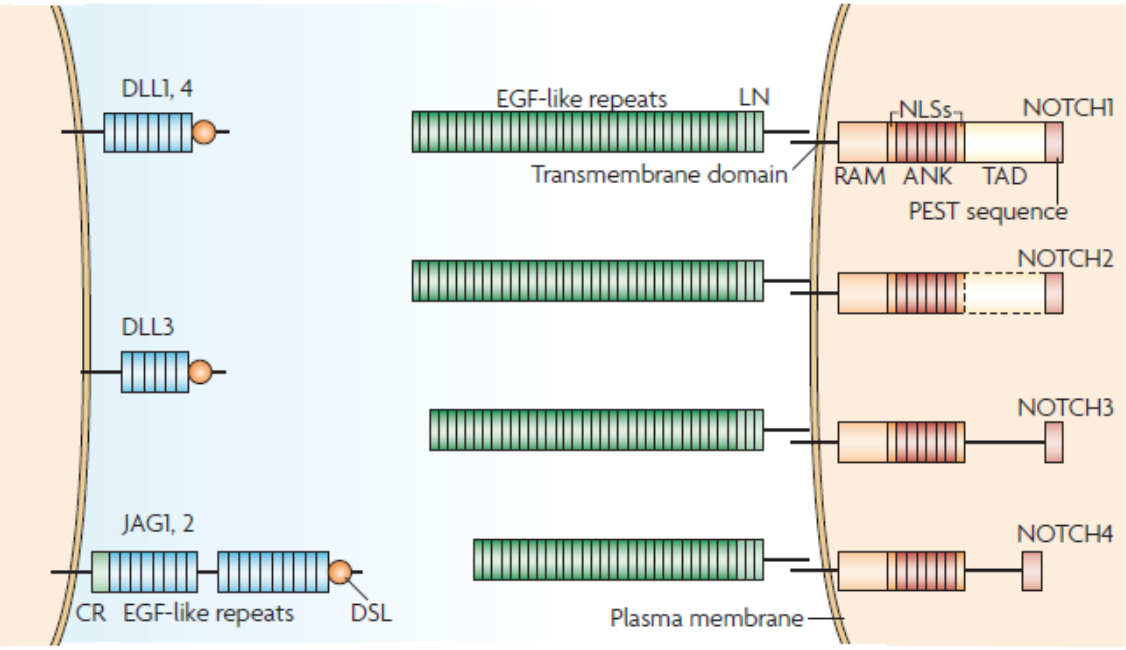

Figure 2: The Delta/Jagged–Notch signalling pathway. On the left, the five transmembrane ligands present in mammals, Delta-like ligand 1 (DLL1), DLL3, DLL4, Jagged 1 (JAG1) and JAG2 are represented. On the right, the four Notch receptors, NOTCH1, NOTCH2, NOTCH3 and NOTCH are shown (12).

The five transmembrane ligands that interact with Notch receptors, Delta-like ligand 1 (DLL1), DLL3, DLL4, Jagged 1 (JAG1) and Jagged 2 (JAG2), share structural homology, including a DSL domain (Delta, Serrate and LAG2), followed by a number of EGF-like repeats (six in the case of DLL3, eight in the case of DLL1 and DLL4, and 18 in the case of JAG1 and JAG2), then a cysteine-rich (CR)

domain found only in JAG1 and JAG2, followed by a transmembrane domain and a small cytoplasmic tail (13).

In figure 3 a typical interaction between a Delta/Jagged ligand and a Notch receptor is shown.

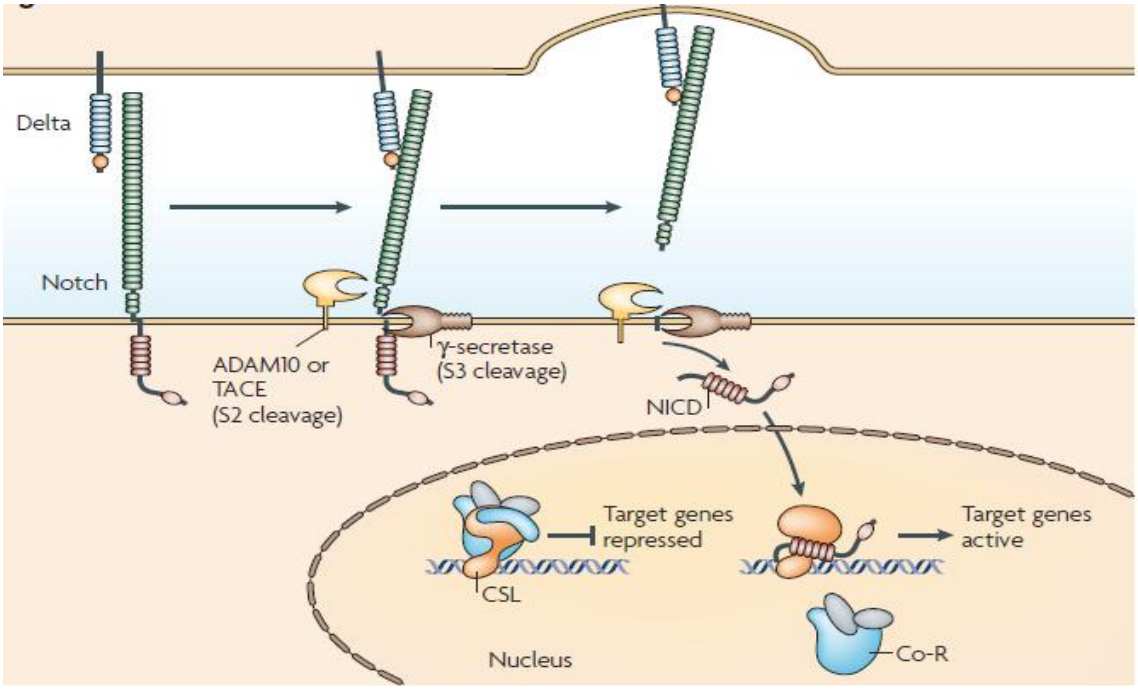

Figure 3: Mechanism of intracellular signaling of Delta/Jagged–Notch pathway (12).

The Delta/Jagged–Notch pathway uses a distinct molecular mechanism to transduce a signal from the cell surface to the nucleus, and thus to regulate expression of target genes. After binding to a Delta ligand, the Notch receptor undergoes a series of proteolytic events near the cell surface, including the S2 cleavage mediated by A Disintegrin And Metalloproteinase 10 (ADAM10) or TNF-α converting enzyme (TACE; also known as ADAM17), followed by the S3 cleavage mediated by the γ-secretase enzyme complex, resulting in the release of the Notch intracellular domain (NICD) which then translocates to the cell nucleus (12). Once in the nucleus, NICD interacts with one of three transcriptional regulators, referred to as CSL, MAML-1, and p300⁄CBP, helping to convert the transcriptional co-repressor (Co-R) complex into an activator complex, and thus induce the expression of a panel of target genes (14,15).

The NICD–RBP-Jk complex up-regulates expression of primary target genes of Notch signaling that belong to the bHLH family. These proteins are characterized by the presence of an Helix-Loop-Helix motif (HLH) and by a DNA binding basic domain (b). In mammals there are two distinct Notch target family:

1) Hes (*Hairy/Enhancer of Split*)
2) HRT (*Hairy-Related Transcription factor*), also known as Hey.

Both Hes and HRT are transcriptional repressors and appear to act as Notch effectors by negatively regulating expression of downstream target genes. Thus, many ligands, receptors, and effectors are involved in this pathway (16).

In addition, two other Notch target genes, the notch-regulated ankyrin repeat-containing protein (NRARP) and Deltex-1 were shown to be potent negative regulators of Notch signaling .

Furthermore, known Notch target genes implicated in cancer are the oncogene c-myc, the transcription factor NF-kB, the cyclinD1 and p21/Waf1(17).

1.2.1 Notch signaling in T-cell acute lymphoblastic leukemia (T-ALL)

The deregulation of Notch pathway in cancer was first described in T-cell acute lymphoblastic leukemia (T-ALL), a neoplastic disorder of the lymphoblast committed to the T-cell lineage. T-ALL represents 15% of childhood and 25% of adult ALL. It is a heterogeneous disease comprising several clinico-biological entities. Cytogenetic analysis of lymphoblasts reveals recurrent translocations activating a small number of oncogenes in 25–50% of T-ALL but a large proportion of T-ALL shows an apparently normal karyotype.

Considering genetic translocations, breakpoints involving TCR loci are recurrent on 14q11 (TCRA/D) and 7q34 (TCRB). During T-cell development with V(D)J recombination taking place, several other genes transcribed at an early stage of thymocyte development are in ‘open’ chromatin configuration and vulnerable to the action of recombinase enzymes. Thus, illegitimate recombinations may juxtapose transcription factor genes and strong promoter and enhancer elements of the TCR genes. This may lead to their aberrant expression in developing thymocytes and give rise to T-ALL with differentiation block at various stages of maturation.

Altogether, translocations involving the TCR loci are found in about 35% of T-ALL with unidentified partner genes in as of yet 5–10% of cases (18).
Cryptic deletions are also frequent and may be concomitant with other changes. The most frequent is loss of the INK4/ARF locus at 9p21 that leads to loss of G1 control of cell cycle (19).
Mutational analysis of oncogenes implicated in T-cell development has shown activating mutations of Notch1 in a high proportion of T-ALL. Indeed, Notch1 is an important player in T-cell assembly and signaling of pre-TCR in immature thymocytes. Moreover, Notch1 could also play a role in differentiation by controlling the turnover of E2A protein. In mice, the absence of the E2A gene products leads to accumulation of double-negative thymocytes. In T-ALL, Notch1 was identified as a fusion partner of TCRB in the rare t(7;9)(q34;q34.3) leading to the formation of N-terminally truncated constitutively active NOTCH1 peptides.
Recently, Notch1 activating mutations have been found in the HD domain and the PEST domain in 56% of T-ALL from all molecular subtypes. Mutations in HD, observed in 44% of T-ALL, result in ligand independent NICD production; mutations in PEST, observed in 30% of T-ALL, extend the half-life of NICD–RBP-Jk transcription activator complex. Combined HD and PEST mutations were found in 17% of cases and were shown to have a synergistic effect on NOTCH1 activation (20). In addition, Notch activation can perturb the balance between apoptosis and survival through different mechanisms. Indeed, Notch1 behaves as a strong repressor of the p53 gene, hence inhibiting pro-apoptotic pathways (21,22). In acute T-ALL cells, the anti-apoptotic effect of Notch signalling is also related to activation of the NFκB pathway (23), regulation of X-linked inhibitor of apoptosis protein (XIAP) stability (24), or suppression of p38 phosphorilation (25).

1.2.2 Normal colon mucosa: a cooperation between WNT and Notch pathway

The colon is comprised of histologically distinct layers, including the mucosa, submucosa, muscle layer, and serosa. The innermost layer consists of a mucosa that includes the epithelium, lamina propria, and a thin layer of muscle. The entire surface of the colonic mucosa is comprised of a functional unit referred to as the crypts of Lieberkühn, which contains approximately 2000–3000 cells (26). The

entire colon contains millions of self-renewing crypts, and it has been estimated that over $6x10^{14}$ epithelial cells are produced during the lifetime of an individual.
Three terminally differentiated epithelial populations are present within the crypt: the **goblet**, the **enteroendocrine** and the **enterocytes** cells. The mucous-secreting goblet and the peptide hormone-secreting enteroendocrine cells belong to the secretory lineage. The enterocytes are members of the absorptive lineage.
Each of these epithelial populations are derived from a pluripotent stem cell located at the base of the crypt (27). The colon stem cells show unique properties as they remain in an undifferentiated state. The stem cells have a long half-life, maintain the ability to self-renew, and have the potential to generate all three differentiated epithelial populations within the colonic crypt compartment. Stem cells usually give rise to two daughter cells by asymmetric division to maintain normal crypt size and homeostasis (28). After division, one cell remains at the bottom of the crypt as a stem cell (self-renewal) and the other cell commits to a transient amplifying cell for subsequent terminal differentiation. Stem cells and transient amplifying cells occupy the lower portion of the crypt (29).
Between colonic stemness markers, Musashi1 (Msi-1) was the first colon stem cell marker to be identified. It was initially reported that Msi-1 is an RNA-binding protein that is indispensable for asymmetric cell division of sensory organ precursor cells in *Drosophila* (30). Msi-1 was also proposed to be required for asymmetric distribution of intrinsic determinants in the developing mammalian nervous system (31). In 2003, Msi-1 positive cells were found in the mouse small intestine (32) and in the human colon at the base of the crypt compartment (33). Studying the function of Musashi-1, it was found that it binds sequence present in the 3'-UTR of the *Numb* mRNA thereby repressing its function at the translational level.
Indeed, Numb protein binds to the ICD of Notch receptor guiding the protein to the degradation pathway (34).

It is well known that the primary driving force behind proliferation and differentiation of epithelial cells in the intestinal crypts is the Wnt pathway. Moreover, Wnt pathway is active in a gradient, with the highest activity at the crypt bottom. However, Wnt signaling is not the only pathway important for colon epithelium

maintenance and differentiation. In fact, the Notch pathway plays a central function in these intestinal cell fate decisions (Figure 4).

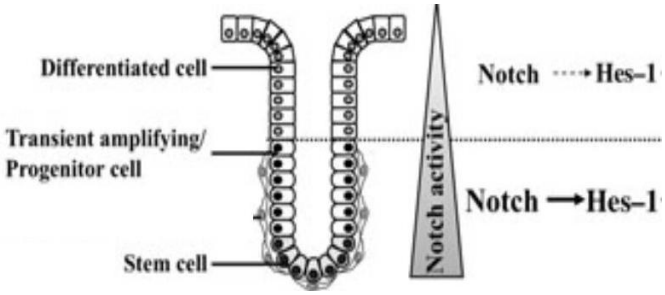

Figure 4: Diagrammatic representation of the colonic crypt compartment and the Notch signaling pathway. Notch activation is observed within the proliferative zone located within the lower region of the crypt (35).

Like Wnt signaling, the Notch pathway is essential to maintain the crypt compartment in its undifferentiated, proliferative state. In the colon, abundant expression of Notch1, Jagged1 and Hes1 was observed in the proliferative zone located within the middle-third of the crypt. On the contrary low level of Notch1 and Hes1 were detected at the apical part of the crypt where differentiated epithelial populations are present (36). The importance for epithelial differentiation was investigated by inhibition of the Notch pathway in the intestinal epithelium by conditional deletion of the CSL gene or through pharmacological γ-secretase inhibitors. The Notch-inhibition results in the rapid and complete conversion of all epithelial cells into goblet cells (37). On the contrary, gain of function through specific over-expression of a constitutively active Notch1 receptor in the intestinal epithelium results in the opposite effect, a depletion of goblet cells and a reduction in enteroendocrine cell differentiation (38).

Specifically, in 2008 *Riccio et al*. shows that conditional inactivation of both Notch1 and Notch2 receptors in the gut results in the complete conversion of the proliferative crypt cells into post-mitotic goblet cells (39). The same effect is seen in intestinal tumors in Apc^{min} mice upon inhibition of the Notch pathway (37).

Looking into details of the genes controlled by Notch during colon differentiation, it has been demonstrated that in the intestine differentiation into **goblet** cells is regulated by Atoh1- kruppel-like factor 4 (Klf4) pathway. Downstream to this

pathway there is activation of expression of the gastrointestinal mucin (*Muc2*). Indeed, Notch target gene *Hes1* represses transcription of the bHLH transcription factor Atoh1, which is directly regulated by Wnt pathway. $Hes1^{-/-}$ animals are embryonic lethal, but intestines from these animals show an increase in goblet, and enteroendocrine cells and a decrease in absorptive enterocytes (40,41).

Likewise, differentiation into **enteroendocrine** cells is guided by Neurogenin3 (Ngn3) that is downstream of the Notch-Hes1-Atoh1 cascade.

Mice homozygous for a null mutation in Ngn3 transcription factor do not develop any intestinal endocrine cells (42).

Finally, **enterocytes** differentiation is driven by E47-like factor 3 (Elf3), which is a target of Hes1 and a member of the Ets transcription family. Indeed, mice homozygous for an Elf3 null mutation die shortly after birth and display poorly polarized enterocytes that have not reached maturity (43).

Thus, all these evidences show that Notch pathway controls absorptive versus secretory fate decisions in the intestinal epithelium (29).

1.2.3 Notch signaling in CRC

Unlike other human tumors no mutational alterations in components of Notch pathway have been reported so far in intestinal tumorigenesis.

Indeed, Notch signaling is aberrantly activated due to mutations of Notch1 in acute lymphoblastic leukemia (see 1.2.1), amplification and over-expression of Notch2 in medulloblastoma (44), chromosomal translocation of Notch3 in lung cancer (45), amplification and over-expression of Notch3 in ovarian cancer (46), and up-regulation of Jag1/Notch1 or down-regulation of NUMB in breast cancer (47) (48).

Together these facts indicate that Notch signaling is oncogenic in a variety of human tumors.

Moreover, in the last years many studies showed that not only in normal colon mucosa, but also in adenoma and CRC there is a cooperation between Apc and Notch pathway.

It was reported that activation of Notch signaling is essential for the development of adenomas in $Apc^{Min/+}$ mice (37) and self-renewal of tumor-initiating cells.

Treatment of $Apc^{Min/+}$ mice with γ-secretase inhibitors resulted in a 50% reduction in the number of intestinal adenomas compared with the vehicle-treated group. Moreover, both the normal-appearing intestinal mucosa and adenomas obtained from γ-secretase treated $Apc^{Min/+}$ mice had increased goblet cell numbers accompanied by a reduction in proliferation when compared with those from vehicle-treated mice. The results indicate that inhibition of Notch signaling increases goblet cell differentiation and reduces proliferation and tumor formation (49). Moreover, Ghaleb *et al*. showed that these effects are mediated by KLF4 transcription factor which they proved to be negatively regulated by Notch signaling (49).

Finally, two different groups Fre *et al*. and Rodilla *et al*. defined the mechanism that mediates the cross-talk between Notch and Wnt pathways in CRC (50,51). Indeed, in these tumors the Notch ligand Jagged1 is directly regulated by β-catenin, thus leading to aberrant activation of Notch1 and Notch2 in CRC (50).

However, already a previous study of Reedijk *et al.* showed that inappropriate activation of Notch signaling occurs colon cancers. Significant up-regulation of Notch1 and Hes1 has been detected in colon adenocarcinomas, but not in normal differentiated epithelial cells by *in situ* hybridization. However, no correlation between *Hes1* expression and survival was found (52).

1.2.4 Notch signaling in the angiogenic process

Studies have implicated that Notch signaling is essential for arterial and venous specification of endothelial cells. Indeed, recent studies in the mouse retina, in zebrafish vessels, in tumor angiogenesis, and in 3D endothelial cell culture sprouting assays demonstrate that the specification of endothelial cells into tip and stalk cells is regulated by Dll4/Notch signaling (53,55). Dll4 is most prominently expressed in tip cells, whereas the strongest Notch signaling activity is regularly observed in the stalk cells (53). Suppression of Notch signaling by γ-secretase inhibitor (GSI) treatment or genetic deletion of one Dll4 allele in the mouse dramatically augments sprouting, branching, and hyperfusion of the capillary network as a result of excessive tip cell formation.

Studies in mouse tumor models illustrated that the principle of tip-stalk specification by Notch signaling is not restricted to developmental angiogenesis, but also controls the branching frequency of tumor blood vessels (54).

Transplantable tumors in Dll4 heterozygous hosts show vastly increased sprouting angiogenesis. Inhibition of Notch signaling by GSI or selective antibody-based blocking of Dll4 leads to similar effects. Analysis of tumor growth provided an intriguing insight into the functional consequences of excessive tip cell formation during sprouting angiogenesis: the increased vascularization after Dll4/Notch inactivation paradoxically causes reduced tumor growth, indicating that unrestrained angiogenesis is unproductive (12). Tracer perfusion experiments demonstrate that the excessive tumor vessels are poorly perfused, causing increased tumor hypoxia and reduced tumor growth. In a converse experiment, increased endothelial Notch signaling triggered by Dll4- expressing tumor cells led to reduced vascular branching and density, but to enhanced vessel diameter, perfusion, and augmented tumor growth (54,56). Together, the developmental and tumor angiogenesis studies support the concept that effective vascular patterning and function require a balance of tip and stalk cell numbers coordinated by Notch (57).

Moreover other studies showed the importance of Notch signaling also in the proliferation of endothelial cell. Suppression of Notch signaling results in increased endothelial cell proliferation in 3D sprouting assays in vitro (55), in mouse and zebrafish development in vivo (53) and during tumor angiogenesis (54). In mouse, increased endothelial cell proliferation of both tip and stalk cells may contribute to increase vessel diameter and branching after GSI treatment (53), after neutralization of Dll4 activity by Dll4-Fc (58), and in $Dll4^{+/-}$ mutants (59).

Taken together these evidences show that Notch signaling is an important regulator of angiogenesis.

1.3 The metastatic process

Whereas surgical resection and adjuvant therapy can cure well confined primary tumors, metastatic disease is largely incurable because of its systemic nature and

the resistance of disseminated tumor cells to existing therapeutic agents. This explains why > 90% of mortality from cancer is attributable to metastases. Thus, our ability to effectively treat cancer is largely dependent on our capacity to interdict, and even reverse, the process of metastasis (60).

The metastases spawned by carcinomas are formed following the completion of a complex succession of cell-biological events, collectively termed the invasion metastasis cascade, whereby epithelial cells in primary tumors: invade locally through surrounding extracellular matrix (ECM) and stromal cell layers, intravasate into the lumina of blood vessels, survive the rigors of transport through the vasculature, arrest at distant organ sites, extravasate into the parenchyma of distant tissues, initially survive in these foreign microenvironments in order to form micrometastases, and reinitiate their proliferative programs at metastatic sites, thereby generating macroscopic, clinically detectable neoplastic growths, often referred to as ‘‘metastatic colonization’’ (61) (Figure 5).

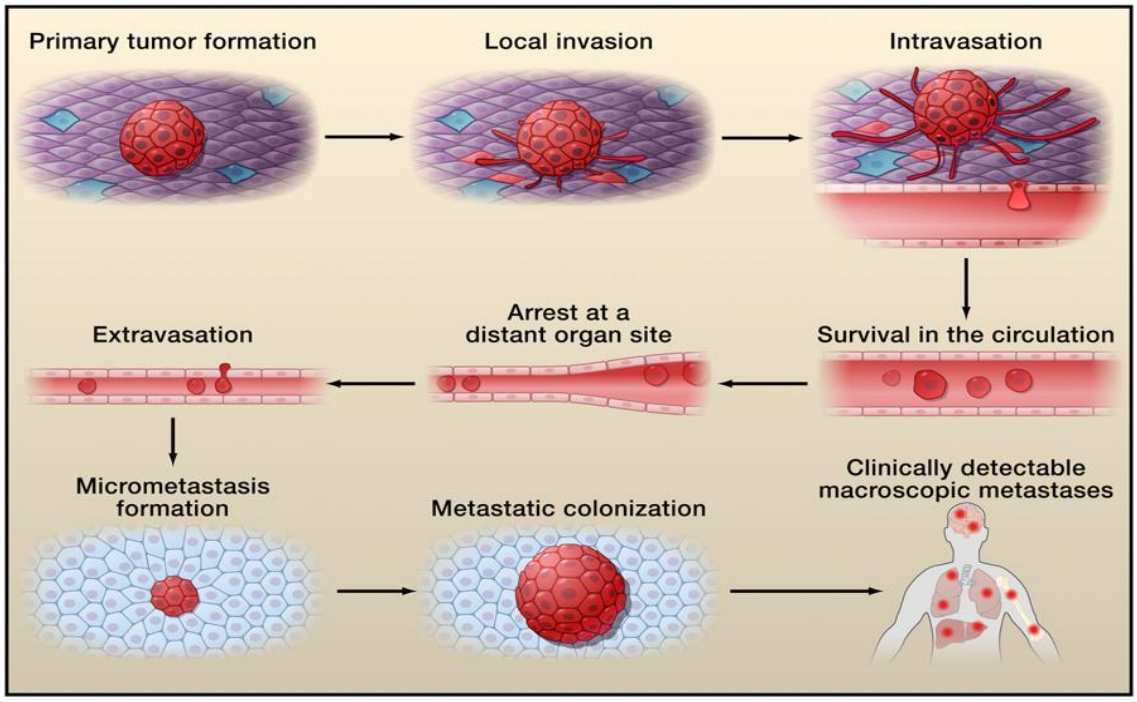

Figure 5: The Invasion-Metastasis Cascade. During metastatic progression, tumor cells exit their primary sites of growth (local invasion, intravasation), translocate systemically (survival in the circulation, arrest at a distant organ site, extravasation), and adapt to survive and thrive in the foreign microenvironments of distant tissues (micrometastasis formation, metastatic colonization)(60).

The invasion-metastasis cascade is extraordinarily inefficient. In fact, some have estimated that < 0.01% of tumor cells that enter into the systemic circulation ultimately develop into macroscopic metastases (62), and this may represent an overestimate.

1.3.1 Local invasion

In order to invade the stroma, carcinoma cells must first breach the basement membrane (BM), a specialized ECM that plays vital roles in organizing epithelial tissues, in part by separating their epithelial and stromal compartments (63).

The epithelial mesenchymal transition (EMT) program, which is critical for multiple aspects of normal embryonic morphogenesis, involves dissolution of adherens and tight junctions and a loss of cell polarity, dissociates the cells within epithelial cell sheets into individual cells that exhibit multiple mesenchymal attributes, including heightened invasiveness (64).

Ultimately, loss of the BM barrier allows direct invasion by carcinoma cells of the stromal compartment. Active proteolysis, effected principally by matrix metalloproteinases (MMPs), drives this loss. Carcinoma cells have devised numerous means by which they derailed the normally tight control of MMP activity, almost invariably leading to enhanced MMP function. While degrading the BM and other ECM that lie in the path of invading tumor cells, MMP-expressing cells also liberate growth factors that are sequestered there, thereby fostering cancer cell proliferation (65).

Once in the stroma, carcinoma cells are enhanced in their aggressive behaviours by stromal cells through various types of heterotypic signaling. For example, breast cancer invasiveness can be stimulated through the secretion of interleukin-6 (IL-6) by adipocytes present in the local microenvironment (66). Furthermore, stromal CD4+ T-lymphocytes promote mammary carcinoma invasion by stimulating tumor-associated macrophages (TAMs) to activate epidermal growth factor receptor (EGFR) signaling in the carcinoma cells (67). Similarly, secretion of IL-4 by breast cancer cells triggers cathepsin protease activity in TAMs, further augmenting carcinoma cell invasiveness (68). These findings provide examples of the bidirectional interactions that occur between tumor cells and the nearby stroma.

Indeed, carcinoma cells stimulate the formation of an inflamed stroma, and the latter enhance the malignant traits of the carcinoma cells, thereby establishing a potentially self-amplifying positive feedback loop (60).

1.3.2 Intravasation

Intravasation involves locally invasive carcinoma cells entering into the lumina of lymphatic or blood vessels. Although lymphatic spread of carcinoma cells is routinely observed in human tumors and represents an important prognostic marker for disease progression, dissemination via the hematogenous circulation appears to represent the major mechanism by which metastatic carcinoma cells disperse (69).

Intravasation can be facilitated by molecular changes that promote the ability of carcinoma cells to cross the pericyte and endothelial cell barriers that form the walls of microvessels. For example, the transcriptional modulator amino-terminal enhancer of split (Aes) inhibits the intravasation of colon carcinoma cells by impairing trans-endothelial invasion through Notch-dependent mechanisms (70).

The mechanics of intravasation are likely to be strongly influenced by the structural features of tumor-associated blood vessels. Indeed, tumor cells stimulate the formation of new blood vessels within their local microenvironment via the process termed neoangiogenesis. However, in contrast to blood vessels present in normal tissues, the neovasculature generated by carcinoma cells is tortuous, prone to leakiness, and in a state of continuous reconfiguration (71).

1.3.3 Survival in the circulation

Once carcinoma cells have successfully intravasated into the lumina of blood vessels, they can disseminate widely through the venous and arterial circulation. Circulating tumor cells (CTCs) in the hematogenous circulation must survive a variety of stresses in order to reach distant organ sites. For example, they would seem to be deprived of the integrin-dependent adhesion to ECM components that is normally essential for cell survival. In the absence of such anchorage, epithelial

cells normally undergo anoikis, a form of apoptosis triggered by loss of anchorage to substratum (72).

In addition to stresses imposed by matrix detachment, tumor cells in the circulation must overcome the damage incurred by hemodynamic shear forces and predation by cells of the innate immune system, specifically natural killer cells (73).

1.3.4 Arrest at distant organs and extravasation

Despite the theoretical ability of CTCs to disseminate to a wide variety of secondary loci, clinicians have long noted that individual carcinoma types form metastases in only a limited subset of target organs. A major unresolved issue concerns whether this tissue tropism simply reflects a passive process whereby CTCs arrest within capillary beds due to the layout of the vasculature and size restrictions imposed by blood vessel diameters or, instead, indicates a capacity of CTCs to actively home to specific organs via genetically template ligand-receptor interactions between these cells and the luminal walls of the microvasculature (60).

The issue of physical trapping of CTCs in microvessels looms can explain the large-scale trapping of colorectal carcinoma cells in the liver, which is dictated by the portal vein that drains the mesenteric circulation directly into the liver (69).

Nevertheless, some CTCs may elude this rapid trapping because of their unusual plasticity or chance passage through arteriovenous shunts, thereby enabling them to become lodged in the microvessels of more distal organs (60).

The alternative hypothesis is that CTCs have predetermined predilections to lodge in certain tissues. Indeed, some carcinoma cells are capable of forming specific adhesive interactions in particular tissues that preferentially favor their trapping. For example entry of colorectal and lung carcinoma cells into the hepatic microvasculature can initiate a proinflammatory cascade that results in Kupffer cells being triggered to secrete chemokines that up-regulate various vascular adhesion receptors, thereby enabling adhesion of CTCs in the microvasculature of the liver (74).

The extravasation would seem to represent, at least superficially, the reverse of the earlier step of intravasation. However, there are reasons to believe that these processes may, in fact, often be quite different mechanistically.

Although intravasation can be fostered by certain co-opted cell types present in the primary tumor stroma, such as the TAMs described earlier (75), these same supporting cells are unlikely to be equally available to facilitate the extravasation of disseminated carcinoma cells. Indeed, macrophage populations that reside in primary tumors are phenotypically and functionally distinct from those present at sites of metastasis formation (76). In addition, the neovasculature formed by primary tumors is tortuous and leaky (71), whereas microvessels in distant normal tissues, the destination sites of disseminated cancer cells, are likely to be highly functional, which can result in low intrinsic permeability.

Hence, the characteristics of specific microenvironments present at metastatic sites may strongly influence the fate of disseminated carcinoma cells. In order to overcome physical barriers to extravasation that operate in tissues with low intrinsic microvessel permeability, primary tumors are capable of secreting factors that perturb these distant microenvironments and induce vascular hyperpermeability, thus creating a “premetastatic niche”.

These findings provide evidence for a model in which extravasation at certain distant organ sites necessitates cell-biological programs that are not required either for intravasation or for extravasation at alternative sites of dissemination, again highlighting the critical role of the specific tissue microenvironments present at possible sites of metastasis formation (60).

1.3.5 Micrometastasis formation

In the event that disseminated carcinoma cells survive their initial encounter with the microenvironment of a foreign tissue and succeed in persisting, they still are not guaranteed to proliferate and form large macroscopic metastases. Indeed, it seems that the vast majority of disseminated tumor cells suffer either slow attrition over periods of weeks and months or persist as microcolonies in a state of apparent long-term dormancy, retaining viability in the absence of any net gain or loss in overall cell number (62).

The concept of “tumor dormancy” comes from several evidences including autopsies of individuals who died of trauma often reveal microscopic colonies of cancer cells, also known as *in situ* tumors. It has been estimated that more than

one-third of women aged 40 to 50, who did not have cancer-related disease in their life-time, were found at autopsy with *in situ* tumors in their breast. But breast cancer is diagnosed in only 1% of women in this age range. Similar observations are also reported for prostate cancer in men.

The realization that a lot of us carry *in situ* tumors, but do not develop the disease, suggests that these microscopic tumors are mostly dormant and need additional signals to grow and become lethal (77). This phenomenon is also often associated with recurrence a long period of time after the removal of the primary tumor. Apparently, metastatic cells start to grow after a period of "dormancy", that can sometimes be measured in years. Recent studies suggest how this condition can be caused either by a circumstance called cellular dormancy because normal cells enter in G0 phase, maintaining their inactivity with a really low metabolism, and becoming quiescent (figure 6a), or because there is an angiogenic dormancy due to poor vascularisation or dormancy due to the immune response (Figure 6b and 6c) (78).

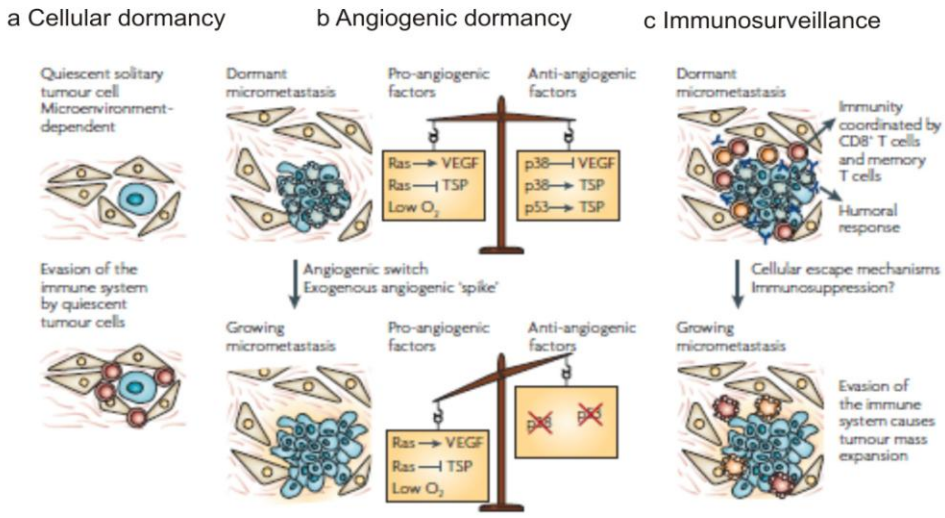

Figure 6: a) During the dormancy stage, sub-clinical disease might be attributed to dormant cells that have entered a G0–G1 arrest (cellular dormancy) and these cells might develop mechanisms to evade immune system recognition and eradication. b) Angiogenic dormancy results from the balance between pro- and anti-angiogenic factors (such as vascular endothelial growth factor (VEGF) and thrombospondin (TSP), respectively). c) Immunosurveillance. Proliferating tumor cells are kept at low numbers (sub-clinical) by an active immune system. This can be due to cytotoxic CD8+ T lymphocytes or anti idiotypic antibodies against the B-cell receptor that arrest the tumor cells (78).

In the case of tumor mass dormancy an important role is played by the ability of tumor cells to induce the generation of new vessels; angiogenic dormancy results from the balance pro- and anti-angiogenic factors, such as vascular endothelial growth factor (VEGF) and thrombospondin (TSP), respectively. Genetic alterations in pathways that maintain angiogenic dormancy or an exogenous angiogenic 'spike' might restore tumor growth. Very often mutations in one of the most important oncogenes are key for the angiogenic switch; for example oncogenic Ras can induce VEGF and repress TSP. By contrast, the stress-activated kinase p38 and the tumor suppressor p53 can induce TSP or repress VEGF. Loss of function of p53 and/or p38 might tip the balance towards enhanced angiogenesis.
In parallel also the immune system is involved in cancer dormancy; proliferating tumor cells are kept at low numbers by an active immune system. An interruption of this state of dormancy might be due to tumor cell escape from immune system control by downregulation of specific tumor-associated antigens or by expression of costimulatory molecules that induce apoptosis of cytotoxic CD8+ T lymphocytes.
Extremely important for the regulation of tumor dormancy seems to be the crosstalk between tumor cells with the microenvironment (78).
In this regard, our laboratory has recently shown the importance of Notch signaling in the escape of human T-ALL cells from dormancy. Indeed, it was shown that escape is associated with Dll4 expression in the tumor microenvironment that increased Notch3 signaling in tumor cells driving these cells to a more aggressive phenotype (79).

1.4 Conventional therapies in CRC

While many patients with early-stage colon cancer (I and II) are cured with surgery alone, the standard of care for stage III and metastatic colon cancer (mCRC) remains a uniform approach to adjuvant chemotherapy.
Conventional adjuvant chemotherapy after chirurgical resection was initially based on 5-fluorouracil, leucovorin and oxaliplatin (FOLFOX4) or 5-fluorouracil, leucovorin and irinotecan (FOLFIRI) or capecitabine plus oxaliplatin (XELOX) only. However,

in the last years clinical trials have shown the benefit of adding bevacizumab (against VEGF-A) or cetuximab or panitumumab (against EGFR) to conventional chemotherapy in the treatment of mCRC (80,81).

Two phase III randomized trials were conducted to test the efficacy of panitumumab with FOLFOX4 or FOLFIRI in the first-line and second-line settings, respectively.

Both trials showed that the addition of panitumumab to chemotherapy significantly improved progression free survival (PFs) but only in patients with wild-type *KRAS* (82,83).

Indeed, for cetuximab and panitumumab only patients with tumors with wild type K-RAS can benefit of the therapy. A retrospective analyses of phase II and III studies have demonstrated that K-RAS mutations are predictive of resistance to anti-EGFR therapies; patients with mCRC with mutant K-RAS tumor status do not derive clinical benefit (84).

Another phase III randomized trials in 2008 was conducted to evaluate the efficacy and safety of bevacizumab when added to first-line oxaliplatin-based chemotherapy either XELOX or FOLFOX4 in patients with mCRC.

This trial showed a statistically significant increase in PFs through the addition of bevacizumab to oxaliplatin-based chemotherapy in first-line mCRC (85).

This indicates the feasibility of combining chemotherapy with upcoming target therapy for CRC.

2. AIMS OF THE STUDY

Colo-rectal cancer (CRC) is the third most frequent tumor in industrialized countries. CRC risk increases with age, but the etiological factors and pathogenetic mechanisms underlying cancer development appear to be complex and heterogeneous. Many studies highlighted the importance of Notch signaling in the differentiation of normal intestinal cells as well as aberrant activation of this pathway in CRC, but the possible contribution of Notch3 has not been investigated before.

Recently, our group described that Notch signaling contributes to regulate tumor dormancy in xenografts of T-ALL and CRC cells. Interestingly, we demonstrated a key role of the microenvironment in triggering Notch activity in tumor cells through up-regulation of DLL4 on tumor-associated endothelial cells.

Starting from these evidences, the first purpose of my PhD work was to investigate whether Notch3 was expressed and regulated oncogenic features of CRC cells. To this end, we investigated expression of components of the Notch pathway (Notch1, Notch3, DLL4, Jagged-1) in human CRC samples both by transcriptome and by tissue microarrays analysis. Moreover, we evaluated effects of Notch3 silencing or over-expression on proliferation of CRC cells in vitro and kinetics of tumor growth in xenograft models.

In the last part of my thesis work I investigated whether Notch3 could be involved also in the formation of lung metastasis in mice. I performed preliminary experiments with a Notch2/3 neutralizing antibody *in vitro* and I evaluated its activity on metastatic growth.

3. MATERIALS AND METHODS

3.1 Cell lines and in vitro culture

The MICOL-14 cell line was derived from a lymph node metastasis of rectal cancer (86) and is poorly tumorigenic following subcutaneous injection into nonobese diabetic severe combined immunodeficient (NOD/SCID) mice; a tumorigenic variant of MICOL- 14 cells, termed MICOL-14t^{um} has been obtained from a tumor developed in NOD/SCID mice after s.c. injection of parental MICOL-14 cells in Matrigel plus bFGF (100 ng/ml; PeproTech,London) and interleukin-8 (100 ng/mL). The MICOL-S cell line was derived from human CRC biopsies (86). All cell lines were grown in RPMI 1640 medium supplemented with 10% FCS and 1% L-glutamine (Invitrogen, Milan, Italy) and used within 6 months from thawing and resuscitation.

To stimulate Notch signalling, P12 wells were coated with soluble recombinant human DLL4 (4 µg/ml) or Jagged-1 (8 µg/ml) (R&D, Minneapolis, MN, USA) in PBS.BSA 0.1%; 1 day later, MICOL-14 cells were added at a concentration of 4□~ 10^4 cells per well in complete medium and cultivated for 72 h prior to subsequent analysis.

To measure proliferation, cells were plated in 96- well plates at a concentration of $3x10^3$ cells per well, and proliferation was evaluated at various time points by the ATP-based ViaLight HS BioAssay kit (Lonza, Basel, Switzerland).

3.2 Patients and Tissue samples

For transcriptome analysis, 20 patients who underwent surgery at the University Hospital of Erlangen at the first manifestation of CRC were included. Patients who underwent preoperative radiation or chemotherapy were not included in this study, nor were patients with familiar CRC or inflammatory bowel disease. Fresh snap-

frozen biopsies were obtained from all patients and used for RNA extraction. Carcinomas underwent histological control for tumor content and cryotomy after manual dissection for tumor enrichment before RNA isolation (87). *In vitro* transcription of the isolated RNA was performed according to the Affymetrix protocols (88). The resulting cRNA was hybridized to Microarrays (HG-U 133A, Affymetrix, Santa Clara, CA). After microarray read out the data analysis was performed with the software Data Mining Tool (Affymetrix). Fold changes (FC) were calculated by comparing the mean signal values between mucosa and tumor of different UICC tumor stages. Significant differences between the groups were calculated using the Mann-Whitney U-test ($P < 0.05$).

In a separate analysis, the commercial Gene Logic (Gaithersburg, MD, USA) database of Affymetrix (Santa Clara, CA, USA) HG-U133 GeneChip expression microarray data (available through Genentech Inc., South San Francisco, CA, USA) was queried for probesets corresponding to Notch1, and Notch3. Signal intensities for the relevant probesets were compared in n=147 normal colorectal mucosa samples, 27 villous adenomas, 77 colorectal cancers and 44 liver metastases.

For tissue microarray (TMA) studies, formalin-fixed and paraffin-embedded tissue blocks and corresponding pathology reports were obtained for 177 sequential patients with CRC undergoing surgery from 1997 to 2000 at the John Radcliffe Hospital, Oxford, UK.

3.3 Tissue Specimens and Cell Isolation

Four hepatic colorectal cancer metastasis specimens were obtained from colon cancer-bearing patients, following informed consent. Immediately after resection, specimens were washed in cold phosphate-buffered saline (PBS) containing Penicillin/Streptomycin, gentamicin (1 µl/ml) and amphotericin (1.25 µg/ml), minced in small pieces and incubated for 3 h at 37°C with collagenase (1.5 mg/ml) and hyaluronidase (20 µg/ml) in DMEM/F12 medium (Gibco, Invitrogen, Carlsbad, CA).

The digested material was centrifuged and sequentially filtered through 70 µm filter. Red blood cells lysis was performed at 37°C for 7' in NH_4Cl/ $KHCO_3$/EDTA buffer. Cell viability was assessed by Trypan Blue dye exclusion. The cell suspension was plated at the concentration of 200.000 cells/well in P12 wells with RPMI 1640 medium supplemented with 10% FCS and 1% L-glutamine (Invitrogen, Milan, Italy). The day before, P12 wells were coated with soluble recombinant human DLL4 (4 µg/ml) or Jagged-1 (8 µg/ml) (R&D, Minneapolis, MN, USA) in PBS.BSA 0.1%; Cells were cultivated for 72 h prior to subsequent analysis.

3.4 Immunohistochemistry (IHC)

For immunohistochemical analysis, 5 µm-thick paraffin- embedded tumor sections were rehydrated and then antigen retrieval was performed by incubation with 0.01 M citrate buffer (pH 6.0) at 95 °C for 20 min. After saturation with 1.5% pre-immune serum, slides were incubated with rabbit anti-HES-1 (Millipore, Billerica, MA, USA), the mouse anti-human Notch3 1E4 antibody (Ab), generated against Notch3 extracellular domain (89), or an anti-activated Notch1 Ab (Ab8925; Abcam, Cambridge, UK), raised against the N-terminus of the Notch1 intracellular domain. For studies in xenografts, rabbit anti-DLL4 Ab reacting with both human and mouse DLL4 (Ab7280; Abcam) was used. For IHC staining of human tumors, a monoclonal anti-DLL4 Ab binding to the extracellular domain of human DLL4 (92) and generated in VelocImmune mice (Regeneron Pharmaceuticals, Inc, Tarrytoen, NY, USA) was used . To investigate Jagged-1 expression, a goat anti-human Jagged-1 Ab (R&D) was used. Basal membrane was stained by a mouse anti-human collagen IV mAb (Clone CIV 22; Dako, Glostrup, Denmark). Cell proliferation was evaluated by staining with the anti-Ki67 antibody (Novocastra Laboratories, Newcastle, UK) or a rabbit anti-phospho-histone H3 Ab (Ser10; Cell Signaling, Danvers, MA, USA), according to the manufacturer instructions. For IHC staining of lung micrometastasis carrying the EGFP gene, a polyclonal rabbit anti-EGFP Ab (Invitrogen) was used. The slides were subsequently washed and incubated with the appropriate secondary Ab. Immunostaining was performed using the avidin-biotin-peroxidase complex technique (Vectastain ABC kit; Vector

Labs, Burlingame, CA, USA), and 3,3'-diaminobenzidine (DAB kit; Dako) was used as a chromogen substrate. Finally, tumor sections were counterstained with Mayer's haematoxylin. The specificity of each staining procedure was confirmed by replacing the primary Ab with PBS.

3.5 Tumorigenicity assay

NOD/SCID mice were purchased from Charles River (Wilmington, MA, USA). For tumor establishment, exponentially growing MICOL-14 and MICOL-14tum cells or their derivatives were washed and resuspended in PBS. Seven- to nine-week-old male mice were injected subcutaneously with $5x10^5$ cells in a 200 µl total volume in both dorsolateral flanks. The resulting tumors were inspected weekly and measured by caliber; tumor volume was calculated by the following formula: tumor volume (mm^3) = L x l^2 x 0.5, where L is the longest diameter, l is the shortest diameter, and 0.5 is a constant to calculate the volume of an ellipsoid. At the end of the experiment, the mice were sacrificed by cervical dislocation; tumors were harvested by dissection and either snap-frozen or fixed in formalin and embedded in paraffin for further analyses.

3.6 RNA extraction, Reverse Transcription and Real-Time PCR Assay

Total RNA was extracted using the TRIzol method according to the manufacturer's instructions. cDNA was synthesized from 0.5-1 µg of total RNA using the Superscript II reverse transcriptase (Invitrogen). Real-time PCR was performed with SYBR Green dye and ABI PRISM® 7900HT Sequence Detection System (PE Biosystems, Foster City, CA). Briefly, fifty-five ng of cDNA were used as a template and mixed with 10 µl of 2X Platinum SYBR Green qPCR SuperMix-UDG (Invitrogen, Carlsbad, CA) and primers in a total reaction volume of 20 µl. Cycling conditions used were 10 min at 95°C, 60 cycles of 15 s at 95°C and 1 min at 60°C. Each sample was run in duplicate. Results were analyzed using the ΔΔCt method

with normalization against β_2-microglobulin (β_2m) expression. PCR efficiency was always in the range 95-105%.
The following primers designed on human transcripts were used:

Primer name	**Sequences**
Notch1 for	5'-GTGCCCTCATGGACGACAAC-3'
Notch1 rev	5'- GCATCCAGGTGCTGCTGAGT-3'
Notch2 for	5'-CAGCCTGTATGTGCCCTGTG-3'
Notch2 rev	5'-GTGCTCCCTTCAAAACCTGCA-3'
Notch3 for	5'-CAAGGGTGAGAGCCTGATGG-3'
Notch3 rev	5'- GAGTCCACTGACGGCAATCC-3'
Dll4 for	5'-AACTGCCCTTCAATTTCACCT-3'
Dll4 rev	5'-GCTGGTTTGCTCATCCAATAA-3'
Jagged1for	5'-TGAATGGGGGTCACTGTCAGA-3'
Jagged1rev	5'-CACCGTTCTGGCAGGGATTAG-3'
Hes-1 for	5'-CAGCGGGCGCAGATGAC-3'
Hes-1 rev	5'-CGTTCATGCACTCGCTGAAG-3'
Hey-1 for	5'-CATACGGCAGGAGGGAAAGG-3'
Hey-1 rev	5'-AACTCGAAGCGGGTCAGAGG-3'
Hey-2 for	5'-GGCGTCGGGATCGGATAAAT-3'
Hey-2 rev	5'-GCGTGTGCGTCAAAGTAGCC-3'
β2-microglobulin for	5'-TGCTGTCTCCATGTTTGATGTATCT-3'
β2-microglobulin rev	5'-TCTCTGCTCCCCACCTCTAAGT-3'

3.7 Western Blot Analysis

Tumor samples were homogenized and cell lysates were run on 7.5-10% polyacrylamide gels; separated proteins were then blotted for 2 h at 400 mA onto a nitrocellulose membrane. The membrane was then saturated with PBS 5% non-fat dry milk (Sigma-Aldrich, St. Louis, MO) as blocking buffer for 1 h at room temperature. Immunoprobing was performed using a rabbit polyclonal antibody (Ab) against the C-terminus of human Notch3 (Ab23426, Abcam, Cambridge, UK), a mouse polyclonal anti-α-tubulin Ab, or a rabbit anti-βactin Ab (Sigma-Aldrich), followed by hybridization with a 1:5000 diluted HRP-conjugated anti-mouse or anti-rabbit Ab (Amersham-Pharmacia, Little Chalfont, UK). Antigens were identified by luminescent visualization using the SuperSignal kit (Pierce, Rockford, IL). Antibodies against α-tubulin or β-actin (Sigma-Aldrich) were used as loading control.

3.8 Immunofluorescence analysis

For immunofluorescence analysis, cells were grown on DLL4-coated Lab-Tek chambers (Nunc, Rochester, NY) for 72 h, fixed, washed 3 times with PBS and then incubated for 1 h at room temperature with a saturating solution consisting of 5% goat serum, 1% BSA, 0.1% Triton-X in PBS. After saturation, slides were incubated with rabbit anti-Notch3 Ab (M134, Santa Cruz Biotech), washed and incubated with appropriate Alexa488-labelled secondary antibodies (Invitrogen). Nuclei were stained with TO-PRO-3 iodide (Invitrogen). Confocal laser scanning microscopy was carried out with a Zeiss LSM 510 microscope (Zeiss, Jena, Germany) using Argon (488 nm) and Helium-Neon (543-633 nm) laser sources. Images were collected at a total magnification of 200 X.

3.9 Reporter gene assay

MICOL-14 cells were transiently co-transfected using lipofectamine 2000 (Invitrogen) with a Notch-responsive luciferase reporter construct - carrying the luciferase reporter gene under the control of a promoter containing CSL binding sites (20) - and a plasmid encoding β-galactosidase under the control of the human CMV promoter, which was used to normalize transfection efficiency. One day later, cells were split and cultivated for additional 48 h on wells coated with human DLL4 (4 μg/ml) or Jagged-1 (8 μg/ml), or bovine serum albumine (BSA) as control. The monoclonal antibodies anti-Notch1 (OMP-52M51), anti-Notch2/3 (OMP-59R5) and the control antibody (CTRL) (OMP-1B711) were kindly provided by *OncoMed Pharmaceuticals Inc.* These antibodies were validated on MICOL-14 or MICOL-14^{tum} cells at 10 μg/ml final concentration per well.

Each experiment was repeated at least three times. Cell lysates were harvested 72h post-transfection and luciferase and β-galactosidase assays were carried out using BriteLite Plus (Perkin-Elmer, Waltham, Massachusetts) and Tropix® Galacto-Light™ (Applied Biosystems), respectively, on a plate luminometer (Perkin-Elmer).

3.10 Transduction of cells with viral vectors

Lentiviral vectors encoding shRNA targeting human *Notch3*, *Notch1* or a scrambled shRNA as a control were purchased from Sigma-Aldrich. The N3ΔE retroviral vectors, encoding constitutively active forms of human Notch3, and the control vector MX-EGFP have been described in detail elsewhere (90). These constructs express membrane-bound Notch3 which is constitutively activated by γ-secretase.

The LV-eGFP vector encoding EGFP protein was used for label MICOL-14 and MICOL-14^{tum} cells in *in vivo* experiments.

Vector stocks were generated by a transient three-plasmid vector-packaging system. For transduction of MICOL-14 or MICOL-S cells, 1 μg of p24 equivalent of concentrated vector-containing supernatant was layered over target cells that had been seeded into 25 cm^2 culture flasks at 7 x 10^5 cells. After 6-9 h at 37°C, the

supernatant was replaced with complete medium. Evaluation of Notch silencing or transgene expression was carried out 72-96 h after transduction.

3.11 Optical imaging of tumors

To perform *in vivo* imaging, tumor cells were transduced with a lentiviral vector encoding the *firefly luciferase* (91) and then injected s.c. into NOD/SCID mice as detailed above. *In vivo* bioluminescence imaging was performed using the IVIS™ Imaging System (Xenogen Corporation, Almeda, CA). Ten minutes before imaging, animals were anesthetized and administered intra-peritoneum (i.p.) with D-luciferin (Biosynth AG, Staad, Switzerland; 150 mg/kg). Signal intensity was quantified as the sum of all detected photon counts (total flux; photons/s) within a region of interest (ROI) prescribed around the tumor sites using the LivingImage® software (Xenogen).

3.12 Statistical analysis

Results were expressed as mean value ± SD. Statistical analysis of the data was performed using Student's *t* -test. Differences were considered statistically significant when $p < 0.05$.
Statistical analysis of TMA data was carried out using PASW Statistics version 18.0 (SPSS Inc, Chicago, IL, USA). Correction for multiple hypothesis testing was performed using the false discovery rate controlling procedure (92).

3.13 Measurement of metastasis area

Quantification of metastatic area in lung sections was carried out by using a light microscope equipped with digital camera (Leica Microsystems) and Leica software (LAS V3.7, Leica). The slides were analyzed at magnification x200 by an experienced pathologist. Results were expressed as mean value of the calculated areas ± SD. Statistical analysis of the data was performed using Student's *t* -test. Differences were considered statistically significant when $p < 0.05$.

4. RESULTS

4.1 Notch3 transcript and protein are expressed in a subset of human CRC samples: results of GEP and TMA analysis

Our interest in understanding whether Notch3 modulates oncogenic features in CRC stems from initial studies performed in primary CRC samples. Both gene expression and TMA analysis showed that Notch3 is up-regulated at the mRNA and protein level in human carcinoma samples compared to normal mucosa.

In figure 1 the mRNA levels of *Notch1* and *Notch3* in normal mucosa, adenoma, primary adenocarcinoma and metastasis are shown. In particular, *Notch3* mRNA was significantly up-regulated in adenocarcinoma and in metastasis compared to matched normal mucosa, whereas it was significantly down-regulated in adenoma compared to normal mucosa. On the contrary, *Notch1* mRNA was significantly up-regulated only in adenoma and in primary adenocarcinoma but not in metastasis.

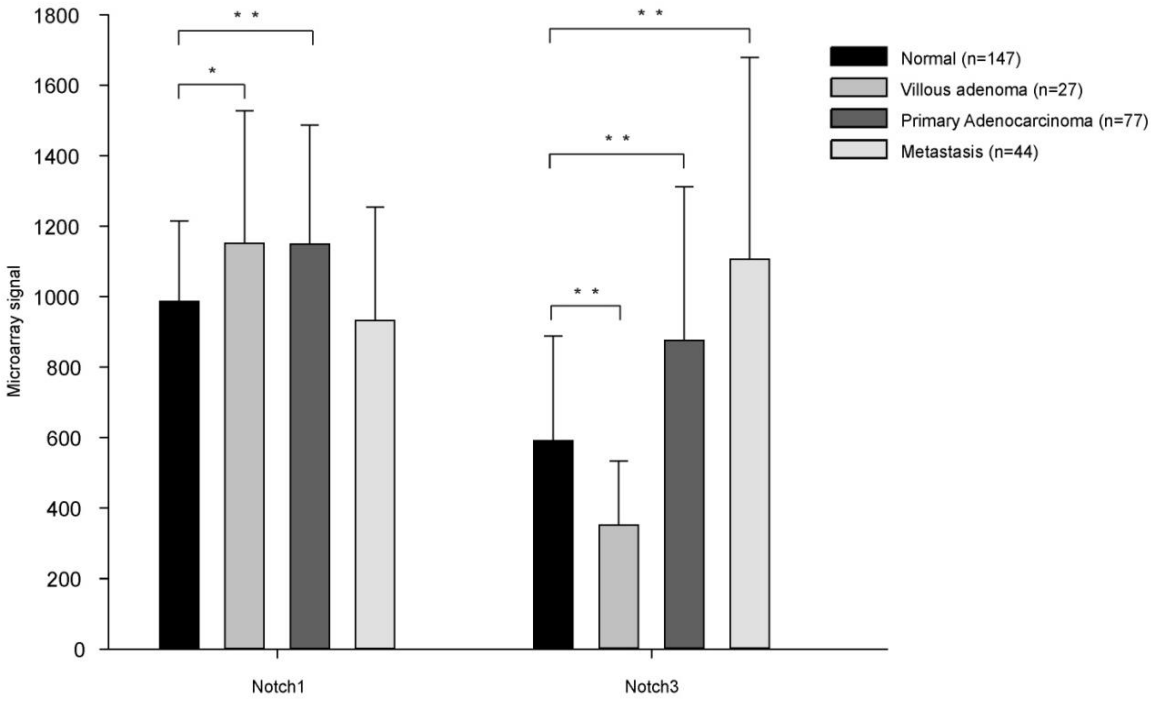

Figure 1: Expression of *Notch1* and *Notch3* transcripts in colon tumors versus normal mucosa by Affymetrix HG-U133 GeneChip expression microarray analysis. Columns show mean ± SD values of expression of *Notch1* and *Notch3* transcripts in the various groups of samples. **p*< 0,05 and ***p*< 0,001, Mann-Whitney Wilcoxon test.

These findings were confirmed by analysis of an independent set of microarray data obtained from twenty CRC samples, stages I–IV, and nine normal controls, which confirmed that *Notch3* levels were significantly up-regulated in CRC versus normal mucosa, independently of stage (Figure 2).

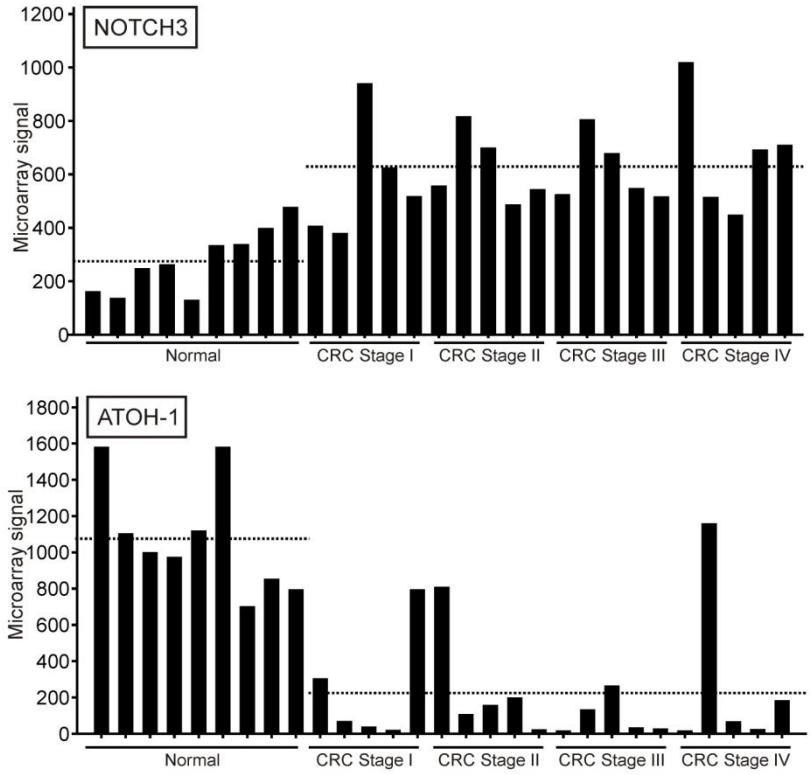

Figure 2: Significant perturbations in *Notch3* and *Atoh-1* RNA levels in CRCs versus normal colon mucosa by HG-U 133A microarray analysis ($p < 0.05$, Mann-Whitney *U*-test). Columns: intensity of probe expression in individual samples; dotted lines: median value for each group of samples.

In this analysis the mRNA of *Atoh-1*, which is a bHLH transcription factor inhibited by Notch, was also considered. Interestingly, *Atoh-1* levels were down-regulated in the majority of CRC samples compared to normal mucosa, thus suggesting activation of the Notch pathway in carcinoma.

In order to confirm these data we stained for Notch1 ICD and Notch3 protein CRC samples (n=158) by using TMA. In figure 3, representative samples with different expression levels of Notch1 ICD and Notch3 are shown. Notch3 has a predominant cytoplasmic staining, whereas Notch1 ICD can be detected both in the cytoplasm and the nucleus. Unfortunately, since the anti-Notch3 antibody recognizes an epitope of the extracellular domain it is not possible to conclude whether strong Notch3 expression correlates with increased activation.

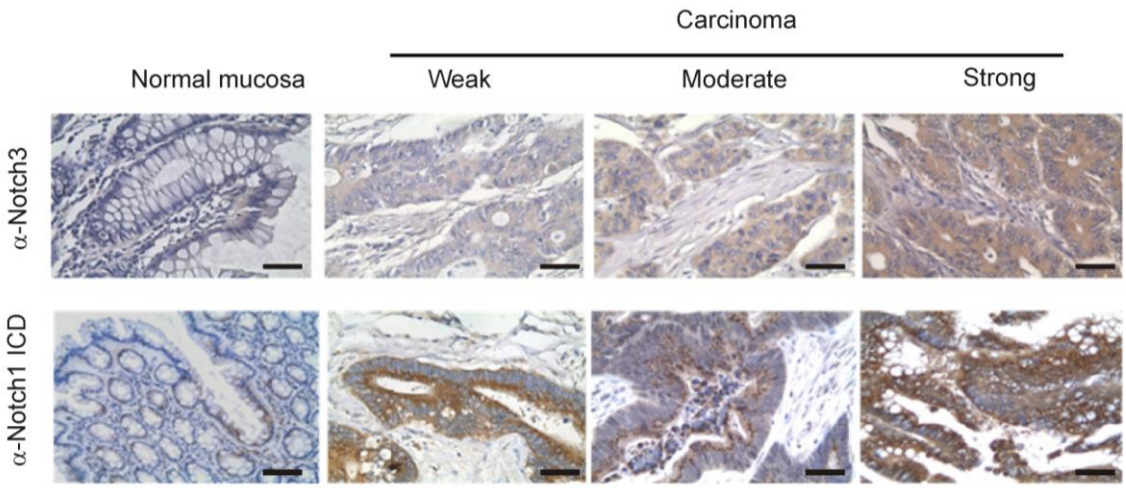

Figure 3: Notch3 (upper panel) and Notch1 ICD (bottom panel) expression in CRCs by IHC. Panels show representative samples with different intensities of staining along with normal colon mucosa. The anti-human Notch3 1E4 Ab and anti-human Notch1 ICD were used. Original magnification ×400**.**

Accurate evaluation and statistical analysis of these samples, disclosed that in normal colon mucosa Notch3 was expressed very rarely by normal epithelial cells, generally with a weak intensity of staining. On the contrary, it was expressed at strong/moderate levels by 19.7% of the CRCs analysed and at weak levels by 51.2% of the samples (Table 1 and Figure 3). Altogether these results show a general up-regulation of Notch3 receptor in carcinoma compared to normal mucosa. Only in about one-third of the CRC samples (29.1%), we could not detect Notch3 by IHC (Table 1).

	Activated Notch1		Notch3	
	Frequency	%	Frequency	%
Tumour	Cytoplasm*			
0	15	4.8	46	29.1
1	29	18.2	81	51.2
2	65	50.3	28	17.8
3	38	26.7	3	1.9
Total	147	100.0	158	100.0
	Nuclear*			
0	126	85.7		
1	21	14.3		
Total	147	100		
Vessels				
0	69	41.8	146	92.4
1	96	58.2	12	7.6
Total	165	100.0	158	100.0

Table 1: Results of IHC staining for Notch1 ICD and Notch3 of CRC TMA.

Moreover, activated Notch1 was detected in almost all samples of CRC analysed and, in particular, at moderate/strong level in 77% of them.
Altogether these data highlight an up-regulation both at the mRNA and protein level of Notch3 and Notch1 in carcinoma samples compared to normal mucosa.
Since Notch3 was still poorly characterized in this context, we focused on the mechanism of Notch3 up-regulation and on its possible oncogenic role.

4.2 Jagged1 and DLL4 expression in TMA CRC samples

In order to investigate the possibility that Notch activity might be regulated by Notch ligands, we analysed their expression in the tumor microenvironment. To this end, we stained for DLL4 and Jagged-1 protein n=158 CRC samples on TMA. Jagged-1 was over-expressed in CRC samples compared to normal mucosa (Figure 4), and it was detected in both malignant epithelial cells and endothelial cells (ECs) (Table 2).

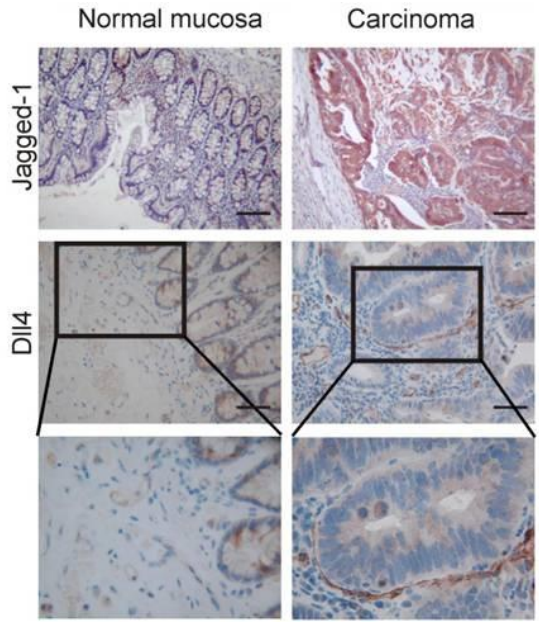

	DLL4		Jagged-1	
	Frequency	%	Frequency	%
Tumour			Cytoplasm*	
0	150	85.7	68	39.3
1	25	14.3	45	26.0
2			59	34.1
3			1	0.6
Total	175	100.0	173	100.0
			Nuclear*	
0			93	53.8
1			80	46.2
Total			173	100.0
Vessels				
0	50	28.6	150	86.7
1	125	71.4	23	13.3
Total	175	100.0	173	100.0

Figure 4 and Table 2: On the left: Expression of the Notch ligands Jagged-1 and DLL4 in CRC. Panels show representative CRC samples along with normal colon mucosa. Original magnification ×200; the boxed areas are magnified (original magnification ×400) to show the proximity between DLL4+ ECs and cancer cells. On the right: Summary of the results of TMA analysis.

In normal colon mucosa DLL4 staining was weak and limited to 10-20% of small vessels; in cancer, however, DLL4 was brightly expressed by the 70 % of all blood vessels present in the section (Figure 4 and Table 2). Notably, the spatial distribution of DLL4+ vessels differed between the two conditions. In normal colon, sporadic DLL4+ ECs were resident in the sub-mucosa, whereas in tumors, DLL4+ vessels penetrated into the tumor mass and were often contiguous to malignant epithelial cells, suggesting possible cell–cell interactions (Figure 4, boxed area). In a subset of samples (14.3%), DLL4 was also expressed by the tumor cells.

In order to understand how the physical interaction between tumor cells and ECs could occur, we evaluated the integrity of the basal membrane. Normal mucosa and CRC samples were stained for Collagen IV (Figure 5) the major structural component of basement membranes. We observed discontinuity of the basal membrane in tumors (black arrows), as opposed to normal mucosa (Figure 5).

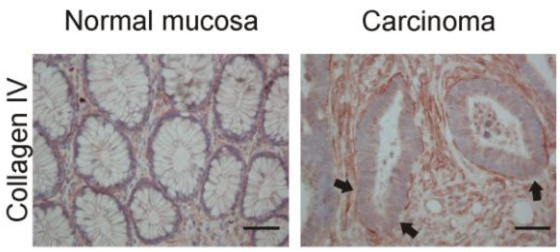

Figure 5: Staining of the basal membrane in tumors or normal mucosa. The basement membrane surrounding epithelial cells, decorated by an anti-human collagen IV mAb, is discontinuous in the tumor sample, whereas it is continuous in the normal mucosa. Original magnification ×250**.**

This discontinuity of the basal membrane in tumor samples could potentially facilitate interactions between DLL4 expressed by the vasculature and Notch receptors in carcinoma cells, thus activating the Notch pathway.

Interestingly, a statistically significant association between DLL4 expression in blood vessels and Notch3 expression at moderate/high levels in tumor cells was noted ($\chi 2 = 8.65$; $p = 0.034$). Moreover, although Notch3 expression in tumor cells did not correlate with Jagged-1 expression in ECs ($\chi 2 = 1.06$; $p = 0.86$), it correlated with cytoplasmic Jagged-1 levels in tumor cells ($\chi 2 = 25.26$; $p = 0.003$).
Finally, the activated form of the Notch1 receptor in the cytoplasm of tumor cells correlated positively with endothelial DLL4 ($\chi 2 = 9.15$; $p = 0.027$) and with Notch3 ($\chi 2 = 27.27$; $p = 0.001$) expression in tumor cells.
Altogether, these results suggest that vascular DLL4 and tumor Jagged-1 ligands could contribute to sustain Notch signalling in CRC.

4.3 Up-regulation of Notch3 is a feature of aggressive CRC xenografts

To further investigate the possibility that signals stemming from the ligands present in the microenvironment might regulate Notch activity in tumor cells, we exploited a xenograft model recently established in our laboratory by using human CRC cells with different tumorigenic properties in NOD/SCID mice. MICOL-14 cells behaved like dormant when injected into the subcutaneous (s.c) tissue of the mice, whereas

the variant termed MICOL-14^{tum} was able to generate large vascularized tumors by 6 weeks from injection (Figure 6A).

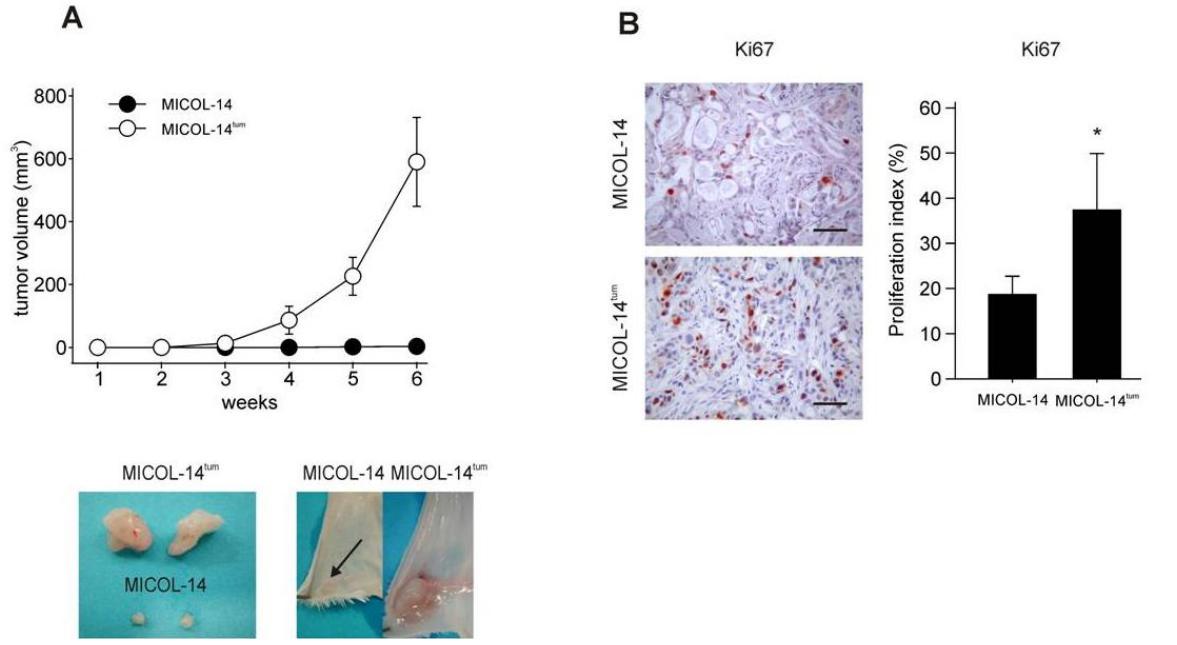

Figure 6: Key features of the MICOL14/MICOL-14^{tum} xenografts. (A) Kinetics of tumor growth following subcutaneous injection of MICOL-14 cells (black dots) and MICOL-14^{tum} (white dots) in NOD/SCID mice (*n* = 5 mice per group). (B) Evaluation of proliferation in MICOL14 and MICOL-14^{tum} tumors. Columns indicate the mean ± SD values of Ki67+ positive cells in *n* = 5–6 samples of each experimental group. *p < 0.05. Left panels show representative images of Ki67+ cells in tumors. Original magnification ×200.

At sacrifice, tumors were paraffin embedded and sections were stained for Ki-67, a marker of proliferating cells (Figure 6B, left). As expected, numbers of Ki67+ cells were significantly higher in aggressive than in dormant tumors (Figure 6B, right). Apoptosis was also evaluated but levels were low and comparable in both tumor entities (not shown). Therefore in this model increased proliferation appears to be a distinctive feature of the tumorigenic variant.

Thereafter, expression of different Notch pathway members was investigated in MICOL-14 e MICOL-14^{tum} tumors both at the mRNA level and at protein level. Expression of several pathway components, including *Notch1*, *Notch3*, *Hes-1*, and *Hey-2*, was markedly increased in MICOL-14^{tum}-derived tumor compared to

dormant tumors (Figure 7A), suggesting that Notch activation is a peculiar feature of aggressive xenografts.

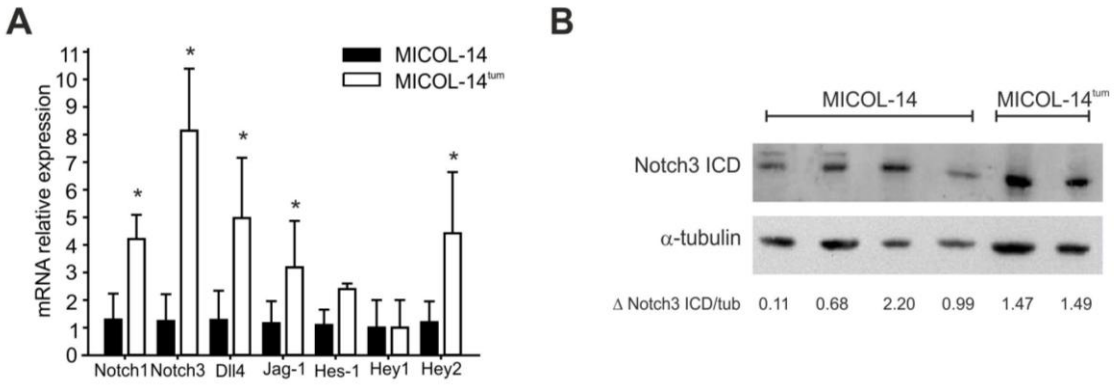

Figure 7: Activation of the Notch pathway in a model of CRC cell dormancy. (A) *Notch1* and *Notch3* transcripts, along with certain Notch target genes (*Hes-1*, *Hey-1*, *Hey-2*) and ligands (*Dll4*, *Jagged-1*), are highly expressed in aggressive tumors by real-time PCR. Columns: means of duplicate determinations in four samples; bars: SD; **p* < 0.05. (B) Variations in Notch3 ICD protein levels in aggressive compared with dormant MICOL-14 tumors. α-Tubulin was used for normalization.

This hypothesis was also reinforced by detection of higher Notch3 ICD levels in aggressive compared to dormant tumors (Figure 7B).

In order to confirm these results we subsequently performed immuno-histochemical analysis of MICOL-14 and MICOL-14^{tum} tumors. As expected, higher expression of Hes-1, DLL4, and Jagged-1 protein was observed in aggressive compared to dormant tumors (Figure 8).

In particular, abundant expression of Jagged-1 and Hes-1 was found in tumor cells, whereas DLL4 was mainly expressed by stromal cells, including both ECs and cells with fibroblast morphology (Figure 8), which is in part reminiscent of what we observed in primary tumor samples.

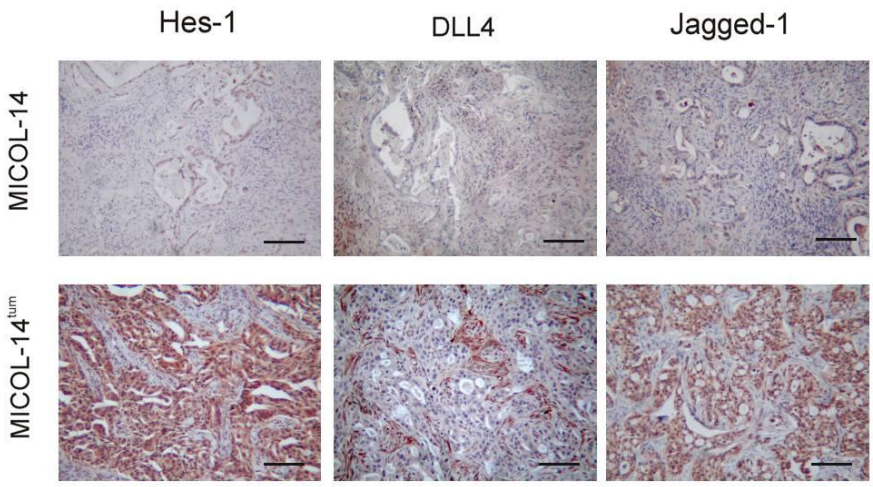

Figure 8: Hes-1, DLL4, and Jagged-1 expression in xenografts of MICOL-14 versus MICOL-14^{tum} cells. Original magnification ×200.

The observation that expression levels of components of Notch pathway are associated with peculiar kinetics of tumor growth convinced us to exploit the MICOL-14/MICOL-14^{tum} model to further investigate how Notch3 expression and activity are regulated.

4.4 DLL4 stimulation strongly induces Notch3 expression

Since both Jagged-1 and DLL4 were found expressed in human CRC samples and in MICOL-14^{tum} xenografts, we investigated the relative potency of these ligands in engaging Notch receptors in CRC cells.

To this end, MICOL-14^{tum} cells were plated on either human DLL4- or Jagged-1-coated wells. After 72 hours of stimulation expression levels of target genes like *Hes-1* and *Hey-2,* together with *Notch1* and *Notch3*, were measured by qPCR.

Both recombinant DLL4 and Jagged-1 increased *Hes-1* and *Hey-2* expression in MICOL-14^{tum} cells, but with different intensity (Figure 9). In these experiments, we also observed a robust (12-fold) increase of *Notch3* mRNA following DLL4 stimulation of MICOL-14^{tum} cells, whereas *Notch1* levels remained substantially unperturbed.

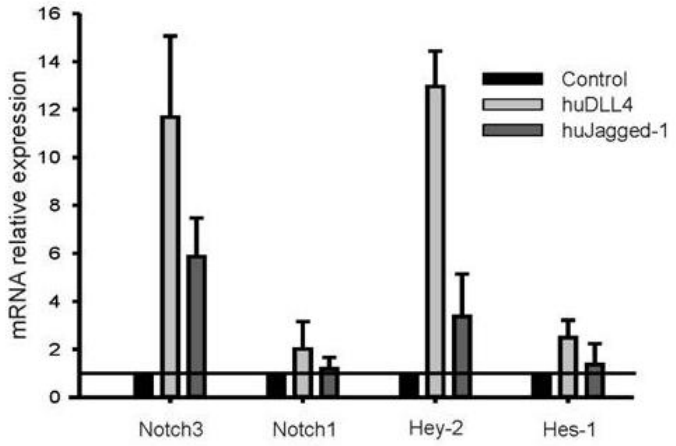

Figure 9: Increased expression of *Notch3* and *Hey-2* in MICOL-14^{tum} cells cultivated for 72 h on recombinant human DLL4 (4 µg/ml) or Jagged-1 (8 µg/ml) by quantitative PCR analysis. Columns: mean values of three independent experiments; bars: SD. *$p < 0.05$.

The observation that DLL4 is a stronger stimulus compared with Jagged-1 was confirmed by a luciferase reporter assay (Figure 10), based on transfection of target cells with a plasmid coding the luciferase gene under the control of a Notch response promoter. After 72 hours of stimulation, luciferase activity was measured with a luminometer. The luciferase signal was normalized on β-galattosidase activity, encoded by a separate plasmid which was co-transfected as internal control of transfection efficiency.

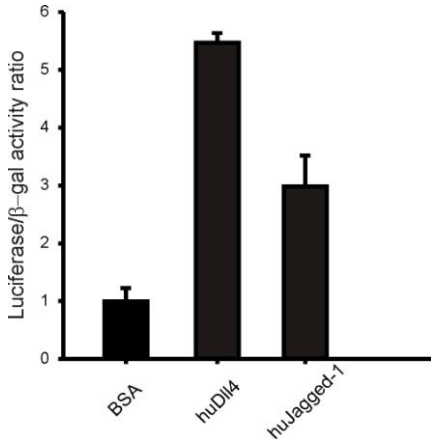

Figure 10: Both DLL4 and Jagged-1 increase Notch activity in MICOL-14 cells by a luciferase reporter assay. The bars represent the mean ± SD of three independent experiments.

Further confirmation was obtained by Immuno-fluorescence (IF) and WB analysis, indicating increased Notch3 full-length and ICD levels in these cells following stimulation with DLL4 (Figure 11 A and B).

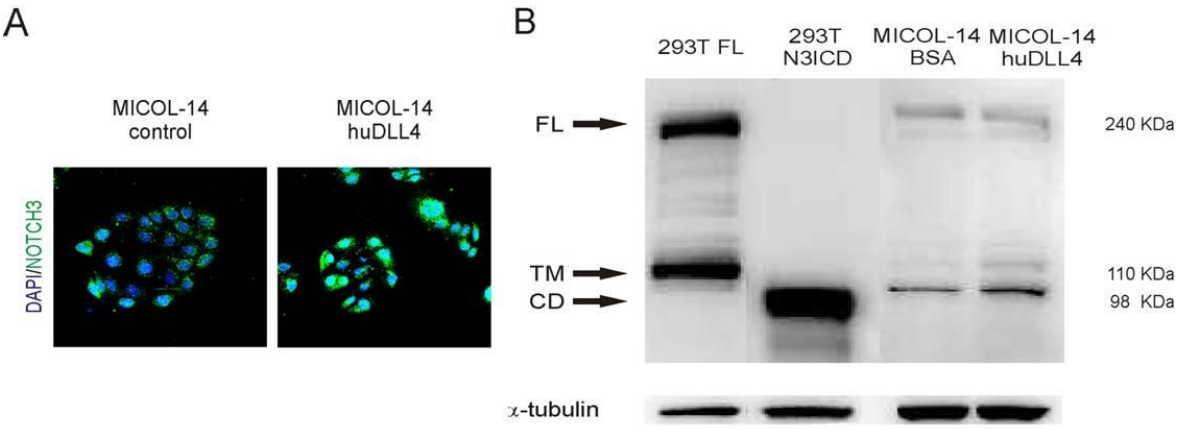

Figure 11: Increased Notch3 expression in MICOL-14 cells following incubation on DLL4-coated wells for 72 h. (A) By IFA using an Ab (M134, Santa Cruz Biotech) to the C-terminus of Notch3 (B) By western blot analysis with rabbit anti-Notch3 Ab (Ab23426, Abcam). The bands corresponding to Notch3 full-length (FL), transmembrane Notch (TM), and ICD following transient transfection of 293T cells with plasmids encoding either Notch3 FL or ICD are indicated by the arrows; α-tubulin was used for normalization.

4.5 Notch3 silencing reduces proliferation in vitro of CRC cells and impairs tumorigenicity

To analyze biological functions of Notch3 in CRC cells, we attenuated its expression by using lentiviral vectors encoding specific shRNAs. Following shRNA delivery, *Notch3* RNA levels were reduced by 60–80% compared to control MICOL-14^{tum} cells (Figure 15A). Notch3-silenced cells displayed a substantial reduction of target gene expression, including *Hes-1* and *Hey-1* and -2 (Figure 12A). Similar results were obtained with a second CRC cell line, termed MICOL-S (Figure 12A).

Notably, Notch3 silencing was followed by a dramatic change in tumor cell morphology. As shown in Figure 12B, MICOL-14^{tum} and MICOL-S cells transduced by the shNotch3 vector displayed a spike-like shape compared with control cells, which maintained a more flattened phenotype. We also measured a moderate, albeit significant, decrease of cell proliferation following Notch3 silencing (Figure 12C, left). Cell cycle analysis of Notch3-silenced cells indicated accumulation of cells in the G0/G1 phase, with corresponding reductions in the S phase (Figure 12C, right).

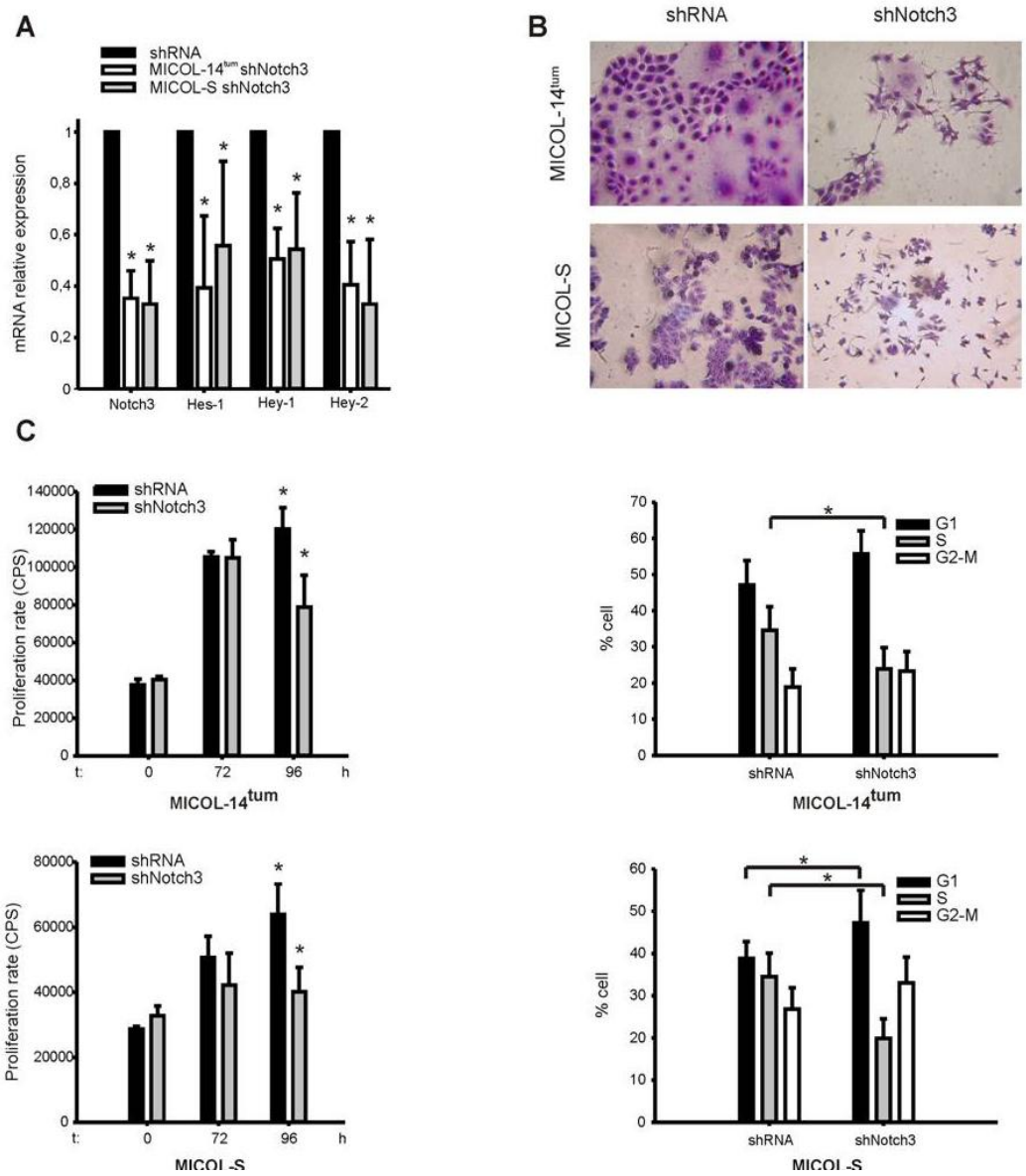

Figure 12: Attenuation of Notch3 levels impairs proliferation of CRC cells and alters their tumorigenic capacity. (A) Reduced expression of Notch3 and Notch target genes in MICOL-14^{tum} and MICOL-S cells transduced by a lentiviral vector encoding a Notch3-specific shRNA (shNotch3) or a control vector (shRNA) by quantitative PCR analysis. Columns: mean values of three independent experiments performed in duplicate; bars: SD. *p < 0.05. (B) Crystal violet staining of MICOL-14^{tum} and MICOL-S cells following Notch3 silencing. Notch3 inhibition led to cytoplasm shrinkage and alterations in cell size and shape. Original magnification ×20. (C) Left panels: proliferation of Notch3 or mock shRNA-transduced cell lines. Notch3 silencing causes a moderate, yet significant reduction of cell proliferation both in MICOL-14^{tum} and in MICOL-S cells 96 h after gene transfer. CPS = counts per second. Columns: mean values of three independent experiments; bars: SD. *p < 0.05. Right panels: effects of Notch inhibition on the cell cycle profile of CRC cells. MICOL-14^{tum} and MICOL-S cells were treated with Notch3 shRNA or control vector (shRNA) for 5 days followed by propidium iodide staining and cell cycle analysis. Columns: mean values of three independent experiments; bars: SD. *p < 0.05.

In accordance with these *in vitro* results, xenograft growth was greatly delayed by Notch3 silencing in MICOL-14^{tum} cells, according to both standard measurements of tumor size (Figure 13A) and optical imaging (Figure 13B).

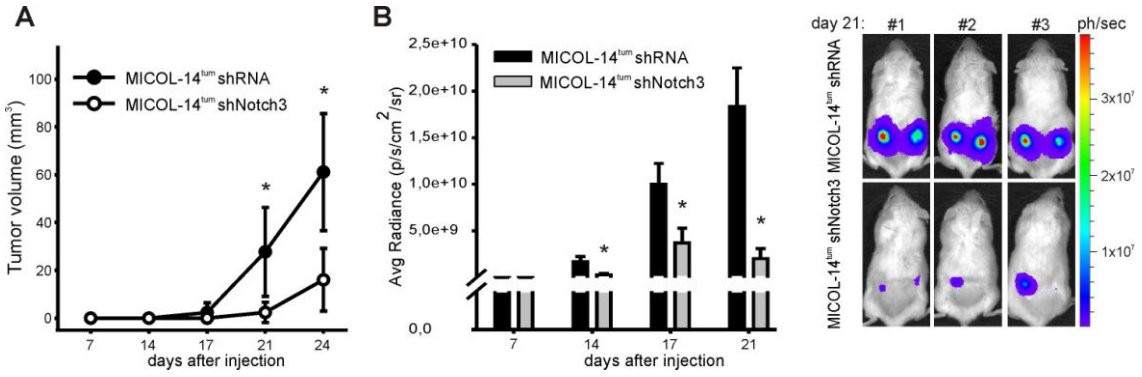

Figure 13: Effects of Notch3 inhibition on tumor growth. (A) kinetics of tumor growth following subcutaneous injection of MICOL-14^{tum} cells transduced by Notch3-specific or control shRNA in NOD/SCID mice (n = 5 mice per group). (B) evaluation of tumor growth by imaging techniques following injection of luciferase-expressing MICOL-14^{tum} cells**.**

4.6 Forced expression of Notch3 in MICOL-14 cells increases *Notch3* and *Hey-2* expression and accelerates tumor growth

Conversely, we asked what could change by forcing expression of Notch3 in "dormant" MICOL-14 cells. We observed that transduction of Notch3ΔE - a constitutively active form of human Notch3 - into MICOL-14 cells increased both *Notch3* and *Hey-2* expression (Figure 14). On the contrary, *Notch1* and *Dll4* transcript levels remained relatively unperturbed following transduction with the Notch3ΔE vector (Figure 14).

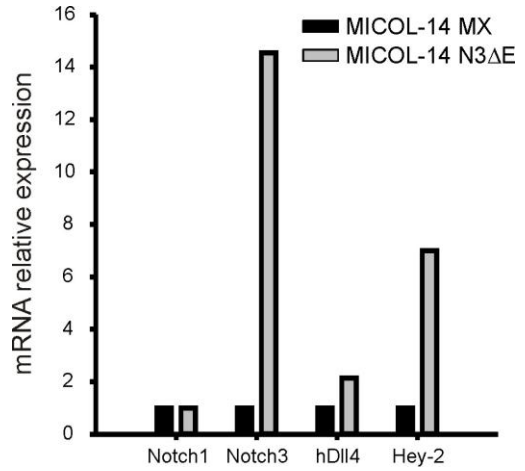

Figure 14: Measurement of transcript levels of components of the Notch pathway in MICOL-14 cells following transduction by a retroviral vector encoding either a ligand-independent active form of Notch3 (N3ΔE) or a control vector (MX). Quantitative PCR analysis was performed 4 days after transduction. One representative experiment out of three performed is shown.

Moreover, MICOL-14 N3ΔE cells showed accelerated tumor growth when injected s.c in NOD/SCID mice (Figures 15A). This result was confirmed by in vivo imaging (Figure 15B). In this case, before injection, MICOL-14 N3ΔE were transduced with a lentiviral vector encoding luciferase (LV-FLuc).

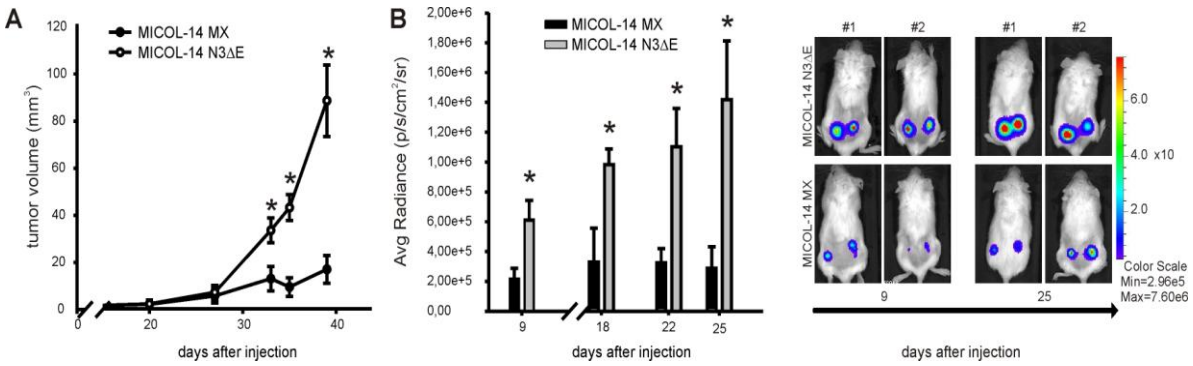

Figure 15: (A) Kinetics of tumor growth following subcutaneous injection of MICOL-14 cells transduced by N3ΔE or control vector (MX) in NOD/SCID mice (*n* = 5 mice per group). (B) Effects of Notch3 over-expression on tumor growth by imaging techniques, following injection of luciferase-expressing MICOL-14 cells.

Following sacrifice, tumor sections were stained for Phospho Histone H, a marker of mitotic cells. Results indicate that proliferation was significantly higher in tumors derived by cells over-expressing Notch3 (Figure 16), indicating that deregulation of Notch3 signaling confers a proliferative advantage to MICOL-14 cells *in vivo*.

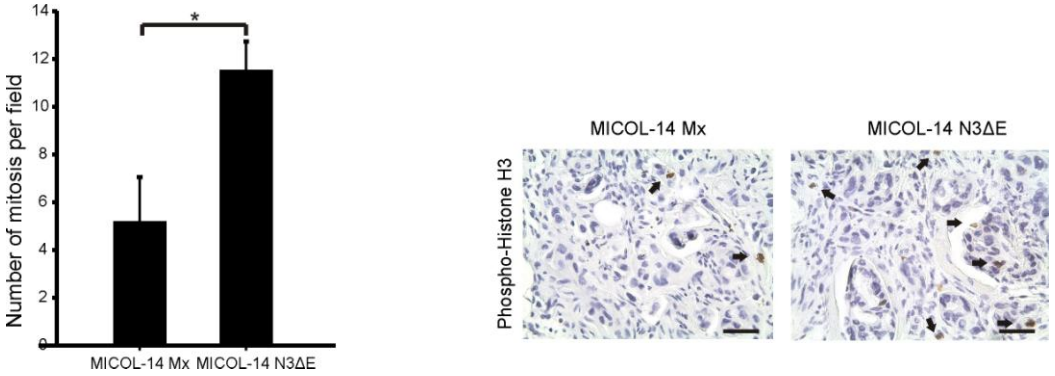

Figure 16: Effects of Notch3 over-expression on cell proliferation *in vivo*. Columns indicate the mean ± SD values of phospho-histone 3 (pH3) positive cells in *n* = 5–6 samples of each experimental group. **p* < 0.05. The right panel shows representative images of pH3+ cells in tumors (arrows). Original magnification ×200**.**

Altogether, these findings indicate that Notch3 levels are crucial to determine the kinetics growth of subcutaneous MICOL-14 xenografts.

4.7 MICOL-14 and MICOL-14^{tum} show different metastatic potential

In order to investigate if the two variants MICOL-14 e MICOL-14^{tum} had a different metastatic potential, we transduced these cells both with a lentiviral vector encoding luciferase (LV-FLuc) and one encoding EGFP (CMV-eGFP). Afterwards, we injected these cells intravenously (i.v) in NOD/SCID mice and we monitored the animals by optical imaging.

As shown in figure 17, MICOL-14^{tum} formed lung metastasis detectable by *in vivo* imaging (Figure 17A) and by IHC analysis against EGFP (Figure 17B). On the contrary, MICOL-14 cells did not form detectable lung metastasis by *in vivo* imaging (Figure 17A). However, micro-metastases were detectable by IHC staining in the lungs of the mice, as shown in figure 17B.

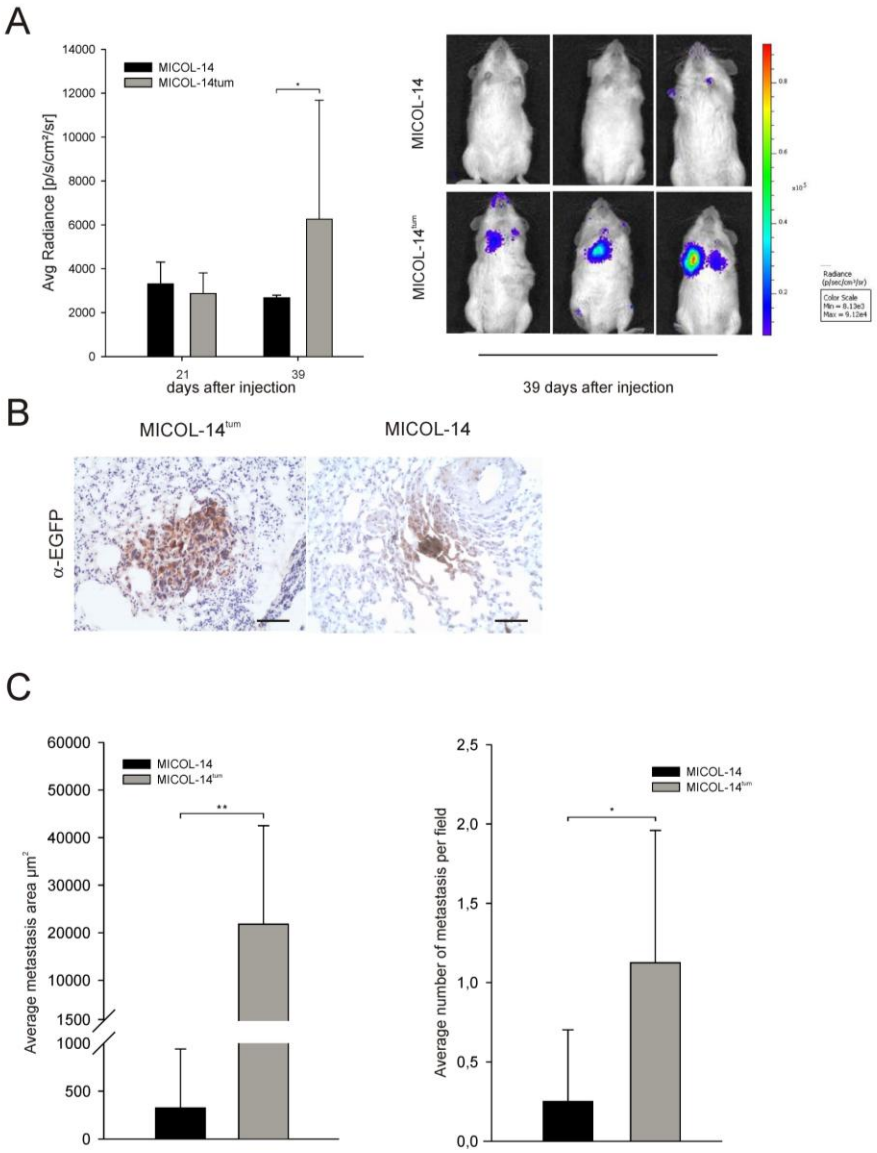

Figure 17: MICOL-14^{tum} cells have a stronger metastatic potential compared to MICOL-14. (A) On the left, kinetics of metastasis growth following intravenous injection of MICOL-14^{tum} and MICOL-14 cells in NOD/SCID mice (*n* = 6 mice per group). On the right, representative imaging of three animals 5 weeks after injection of MICOL-14 or MICOL-14^{tum} cells. (B) A representative IHC staining against EGFP epitope in MICOL-14^{tum} and MICOL-14 metastasis of the lung. Original magnification ×200. (C) On the left, columns indicate the average of metastatic area of MICOL-14 versus MICOL-14^{tum} , in *n* =12/13 samples per each experimental group. There is a significantly difference between the two groups *$p < 0.001$. On the right, columns indicate the average number of metastasis per sections of MICOL-14 versus MICOL-14^{tum} in *n* = 21 slides per each experimental group. There is a significantly difference between the two groups *$p < 0.05$.

We performed also a quantitative analysis evaluating the average area and the number of metastases in both experimental groups. As expected, both size and number of metastases was significantly different in the two groups (Figure 17C).

Collectively, these data indicate that MICOL-14^{tum} cells have stronger metastatic potential to the lungs compared to MICOL-14 cells in NOD/SCID mice.

4.8 Antibody-mediated neutralization of Notch3 exerts similar effects to Notch3 silencing

In the last part of the study, we evaluated effects of an anti-Notch2/3-specific antibody in CRC cells. We obtained an antibody against the extracellular domain of both Notch2 and Notch3 receptors, kindly provided by *OncoMed Pharmaceuticals Inc.*, a US-based company. Initially, we transfected target cells with a plasmid coding the luciferase gene under the control of a Notch response promoter. Thus, we validated the activity of this antibody by performing an *in vitro* luciferase reporter assay. As expected, we observed that the anti-Notch2/3 antibody decreased Notch activity of hDLL4 stimulated cells to basal levels in both cell variants (Figure 18).

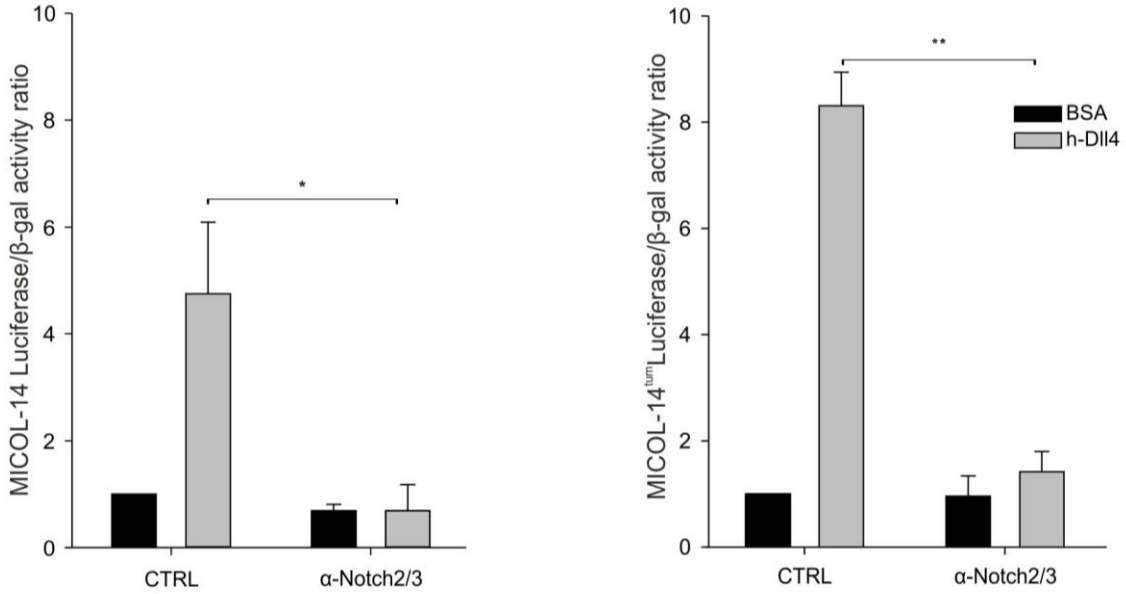

Figure 18: Luciferase activity in MICOL-14 or MICOL-14^{tum} after stimulation with hDLL4 (grey bars) and treated with anti-Notch2/3 or control antibody. Luciferase activity was measured 72h after treatment. *p< 0,05 and *p< 0,001.

Moreover, to confirm the role of Notch3 in these cells we performed similar experiments by using an antibody blocking Notch1 receptor (Figure 19). As expected, we observed that in MICOL-14^{tum} cells the anti-Notch1 antibody, unlike the anti-Notch2/3, did not decrease Notch activity of hDLL4 stimulated cells to basal levels.

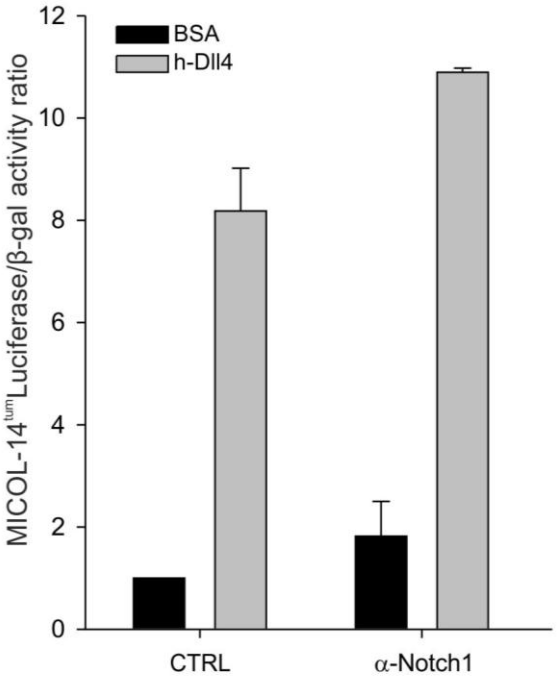

Figure 19: Luciferase activity in MICOL-14^{tum} after stimulation with hDLL4 (grey bars) and treated with anti-Notch1 or control antibody. Luciferase activity was measured 72h after treatment. One representative of three experiments is shown.

These data were subsequently confirmed by measurement of transcript levels of endogenous components of the Notch pathway. Indeed, following stimulation with hDLL4 and incubation with the anti-Notch2/3 antibody, mRNA level of *Hey-2* significantly decreased in both MICOL-14 and MICOL-14^{tum} (Figure 20) compared to control. Moreover, in MICOL-14^{tum} cells we observed an up-regulation of *Notch3* mRNA after DLL4 stimulation, which was blocked by the addition of the anti-Notch2/3 antibody. Similar effects at the mRNA level were previously observed after attenuation of *Notch3* expression by using lentiviral vectors encoding specific shRNA (Figure 12A).

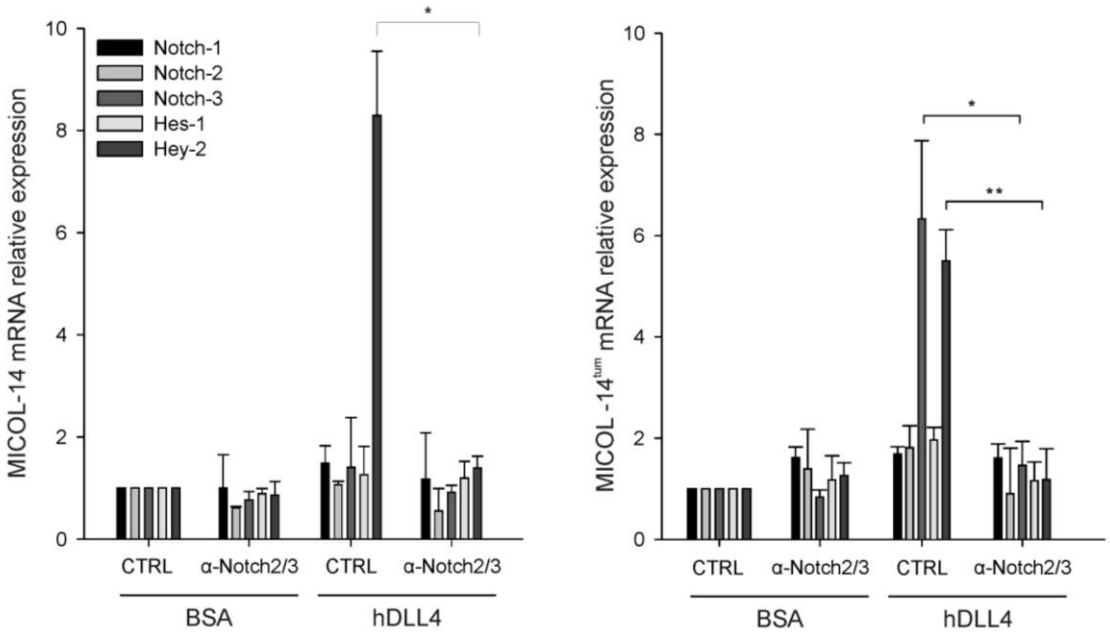

Figure 20: Levels of components of the Notch pathway in MICOL-14 and MICOL-14^{tum} cells, following stimulation with hDLL4 and incubation with anti-Notch2/3 or control antibody. Quantitative PCR analysis was performed 4 days after treatment. Average of three independent experiment is shown.

Furthermore, the effects of the anti-Notch2/3 antibody were also investigated in three hepatic metastasis derived from patient with CRC (Figure 21). By gene expression analysis we observed a reduction of Notch target genes after incubation with anti-Notch2/3 antibody.

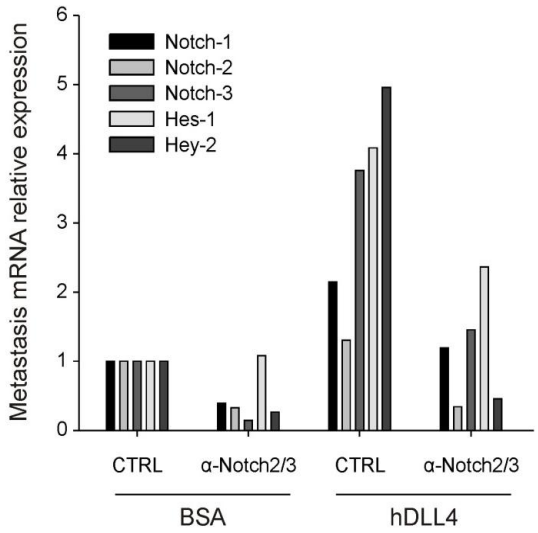

Figure 21: Reduction of Notch target genes after 96h stimulation with hDLL4 and incubation with anti-Notch2/3 antibody in one hepatic metastasis derived from a patient with CRC. One representative of three independent experiments is shown.

Collectively, these data indicate that this antibody is able to recognize its target and blocks Notch signaling in CRC cells, inducing similar transcriptional effects to the attenuation of Notch3 expression by using shRNA.
Since, the anti-Notch2/3 antibody is able to bind also to the Notch2 extracellular domain, it is not possible at the moment to exclude the contribution of Notch2 receptor to these results.

4.9 Preliminary data of lung metastases treatment with anti-Notch2/3 antibody

Supported by our previous results and intrigued by the different metastatic potential of MICOL-14 and MICOL-14^{tum} cells, we wondered if the inhibition of Notch3 protein *in vivo* could delay the growth of MICOL-14^{tum} metastases. To this end, we performed a preliminary experiment consisting in treatment with anti-Notch2/3 antibody of mice carrying lung metastases generated by i.v injection of MICOL-14^{tum} cells.

Initially, as shown in figure 22, we looked at the presence of our target in the metastases. Therefore, we stained for EGFP and Notch3 protein lung metastases derived from the i.v injection of MICOL-14^{tum} cells encoding EGFP protein in NOD/SCID mice.

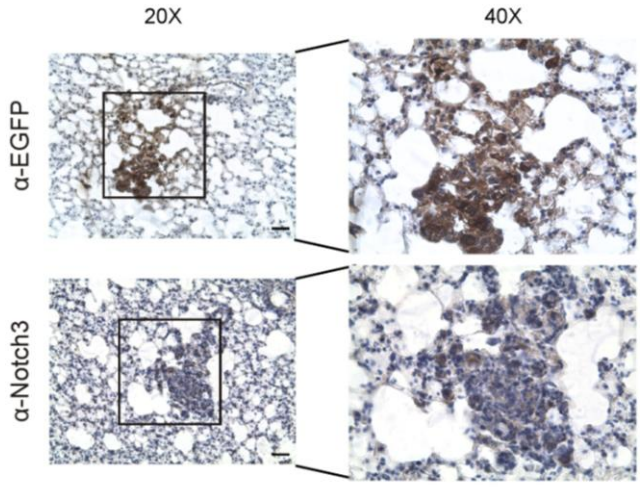

Figure 22: Upper panel, IHC staining for EGFP to localize lung metastasis. Bottom panel, IHC for Notch3 protein to confirm presence of our target in lung metastasis. Six of ten metastasis analyzed stained positive for Notch3.

Six of ten metastases stained positive for Notch3 protein, suggesting that this protein is expressed not only by primary s.c tumors but also in the metastatic context.

Afterward, we performed a preliminary experiment in which, after the first positive imaging (Figure 23B), we started treatment of five versus five NOD/SCID mice carrying lung metastases. Mice were injected intra-peritoneal (i.p) with anti-Notch2/3 antibody or control (400 µg/mouse), once a week, for the period of one month. The scheme of the treatment is shown in figure 23A.

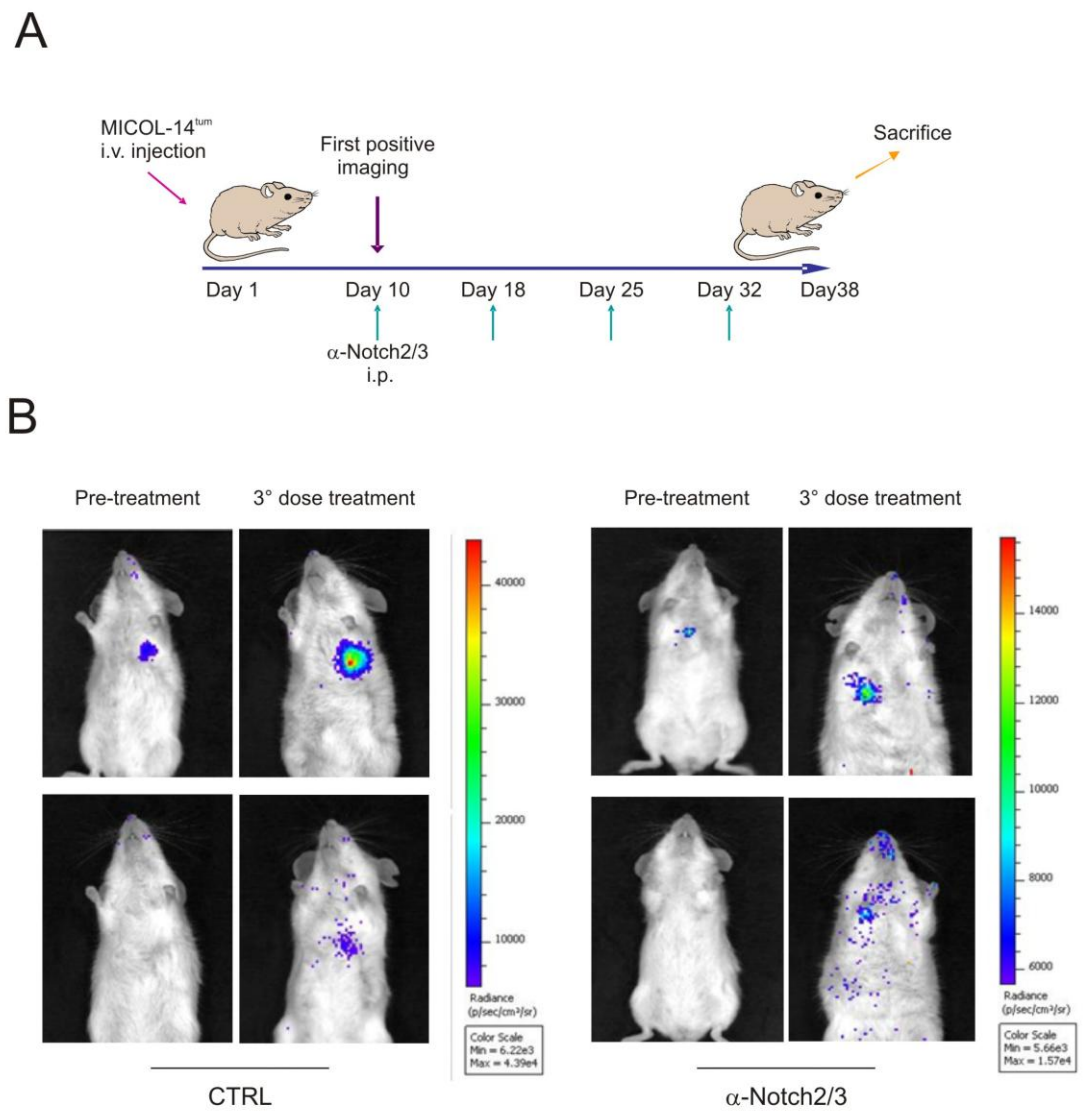

Figure 23: Preliminary results of lung metastasis treatment with anti-Notch2/3 antibody. (A) Scheme of treatment with anti-Notch2/3 or control antibody of NOD/SCID mice carrying lung metastasis derived from the i.v injection of MICOL-14^{tum} cells. (B) *in vivo* imaging of two representative mice per experimental group. The images show the metastatic areas before the treatment and after three dose of anti-Notch2/3 or CTRL.

From the *in vivo* imaging (Figure 23B) we observed that treatment with anti-Notch2/3 antibody (Figure 23B, right panel) did not block the progression of metastasis, even in mice that at the beginning of the therapy did not show any detectable metastasis signal. However, we observed that the intensity of the signal is lower in treated mice versus control (Average AvgRadiance anti-Notch2/3

3,83E+03 ± SD 332,3402; Average AvgRadiance control 5,35E+03 ± SD 1775,545).

At the sacrifice, lungs were explanted and IHC staining for EGFP, to localize lung metastases on 20 lung sections per group obtained at different depth, was performed. Subsequently, we evaluated the average area and the number of metastases in both experimental groups (Figure 24). We observed that both size and number of metastases were not significantly different between the two groups, although in anti-Notch2/3 treated mice there is a trend that suggests a reduction of both size and number of metastases (Figure 24).

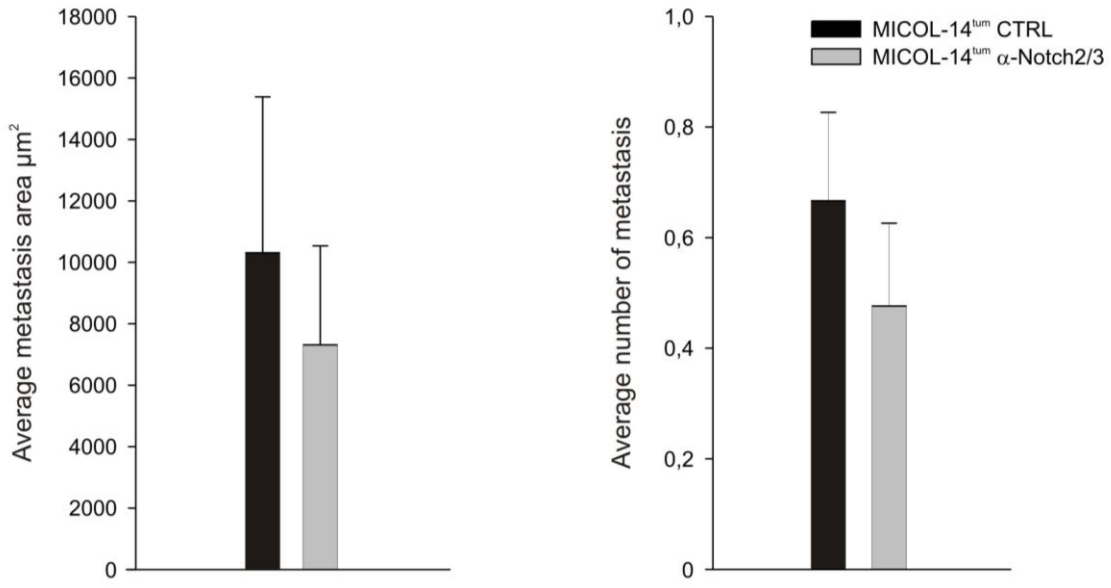

Figure 24: Average area (on the left) and the number of lung metastases (on the right) in both experimental groups are shown. 5 lung per group were considered for the quantitative analysis and *n*= 20 lung sections per group. The error bar is representative of the standard error.

Ongoing experiments are aiming at measuring levels of Notch signalling in the *ex vivo* samples, in order to determine whether Notch signalling was reduced by the antibody activity in this experiment.

5. DISCUSSION

Colo-rectal cancer is the third most frequent malignancy both in men and women after prostate or breast cancer respectively, and lung cancer (1). The molecular pathways dis-regulated in CRC are complex and heterogeneous. In the last years, however, the importance of cooperation of Wnt and Notch in CRC development has been highlighted by many studies.

Several studies reported expression of components of the Notch pathway in colon adenoma and cancer. Some of them highlighted a cross-talk between Notch and the WNT/β-catenin mediated by Jagged-1. This Notch ligand is a target of β-catenin signalling and appears to be important in driving Notch1 activation in adenoma cells (37,50,52), although its role in cancer is not yet firmly established. Moreover, the contribution of other Notch receptors in CRC remains poorly investigated.

In this study we proposed that Notch3 contributes to Notch signalling in CRC cells by a crosstalk involving stromal cells expressing the DLL4 ligand. The study was initially stimulated by the observation that, in two different GEP datasets, the *Notch3* transcript was significantly higher in CRC samples and in metastasis compared to normal mucosa, together with a decrease in *Atoh-1* expression, which is known to be inhibited by Notch signalling (40).

Afterwards, we showed that Notch3 is expressed by 70% of CRC samples and in almost 20% of cases with strong-moderate intensity. Moreover, we showed that DLL4 is abundantly expressed by the tumor vasculature, whereas it was weakly expressed in normal colon mucosa. These findings suggest the possibility that Notch3 activation in CRC cells is triggered by cell–cell interactions involving DLL4+ endothelial cells and Notch3+ cancer cells.

Intriguingly, this hypothesis is supported by the observation that in tumor samples there is a discontinuity of the basal membrane surrounding tumor pseudo-glandular structures that was not detected in normal colon mucosa.

Furthermore, statistical analysis of TMA data disclosed a positive correlation between DLL4 and Notch3 expression in tumors.
Collectively, these data suggest that DLL4 expressed by tumor vasculature contributes to regulate Notch activity in CRC cells, as also recently shown in pre-clinical models of T-ALL (79).
Since DLL4 levels are regulated by VEGF in EC (93) and correlate with VEGF expression in CRC samples (92), it is tempting to speculate that Notch activity might be particularly strong in highly angiogenic tumors.

Functions of Notch3 in CRC cells were investigated in a xenograft model of CRC. Indeed, the higher tumorigenic potential of MICOL-14^{tum} compared with MICOL-14 cells was associated with marked activation of the Notch pathway and expression of DLL4 in MICOL-14^{tum} xenografts, fitting our previous observations in other models of tumor dormancy (79). *In vitro* experiments disclosed up-regulation of both Notch3 mRNA and protein after stimulation of MICOL-14^{tum} and MICOL-14 cells with recombinant human DLL4, followed by increased Notch signalling detected by a Notch-reporter assay.
Overall, these *in vitro* findings agree with the results of our TMA studies which showed a positive association between DLL4 expression and activated Notch3 protein. However, the contribution of other ligands cannot be excluded. Indeed, we found increased expression of Jagged-1 both in mice xenografts and in human CRC samples. These results substantially agree with previous studies which showed increased expression of Jagged-1 either in normal mucosa and in colon cancer (50,52). In mice studies, Jagged-1, whose expression is in part controlled by the WNT/β-catenin pathway, was considered the main driver of Notch1 activation in colon adenomas, and we also found that Jagged-1 activates Notch signaling in CRC cells, albeit less efficiently than DLL4. In this respect, the results of our TMA studies indicate that Jagged-1 expressed by the tumor rather than stromal cells is correlated with Notch3 expression levels.

Although in this study we focused on regulation of Notch3 expression and activity by DLL4 and Jagged-1, it is important to be aware of alternative explanations for our findings. With regard to the mechanisms causing Notch3 over-expression and

activation, to the best of our knowledge, mutations of Notch pathway components in CRC samples have rarely been report (94,95). Among other potential genetic mechanisms, Notch3 gene amplification has been currently reported in low percentage in breast cancer (96) and in ovarian cancer (46), therefore in our samples we cannot exclude whether Notch3 gene copy number is also increased in cancer compared with normal colon mucosa. To this regard, we recently detected amplification of the *Notch3* gene in 2 of 16 CRC samples, compared to matched normal mucosa (data not shown). In any case, analysis of a larger number of CRC samples will be necessary to confirm this result.

Finally, we showed that Notch3 levels are critical for generation of xenografts of CRC cells in mice. Indeed, *in vitro* results demonstrated a slight decrease in proliferation and accumulation of cells in the G0/G1 phase after *Notch3* silencing. Moreover, in agreement with these *in vitro* results, *Notch3* silencing impairs xenograft tumor growth of MICOL-14^{tum} cells.
These effects are in line with those reported by other groups following genetic inactivation of Notch3 in ovarian, lung and breast cancer cells (46,96,97), and they may reasonably explain why silencing Notch3 weakens the tumorigenic potentiality of MICOL-14^{tum} cells and induces tumor dormancy. On the other hand, forced expression of the active form of Notch3 increased proliferation and kinetics of growth of MICOL-14 subcutaneous xenografts.

Furthermore, we investigated the metastatic potential of MICOL-14 and MICOL-14^{tum} cells by injecting these cells intravenously in NOD/SCID mice. We found that MICOL-14^{tum} cells generated a larger number of lung metastases compared to MICOL-14 cells. Moreover, IHC staining showed that Notch3 was expressed by the majority of the metastases formed by MICOL-14^{tum} cells.
Unexpectedly, however, we were unable to reduce metastatic burden after treatment of mice bearing MICOL-14^{tum} lung metastasis with an anti-Notch2/3 antibody, which efficiently reduced Notch signaling in these cells in vitro.
Current experiments are finalized to clarify whether Notch signaling was effectively reduced by anti-Notch2/3 administration *in vivo*, or whether the administration schedule needs to be intensified. A complementary experiment aiming to test the

metastatic potential of MICOL-14^{tum} bearing shRNA-reduced *Notch3* levels is also ongoing. Moreover, although it is an unlikely hypothesis due to the relatively short duration of treatment, we cannot exclude the possibility of a transient inhibitory effect surmounted by development of secondary resistance to Notch inhibition. Indeed, several studies indicate the possibility of resistance to the target therapy, for example correlated to the administration of anti-EGFR antibodies to CRC patients with mutated KRAS (84).

Alternatively, these negative findings might underscore that Notch signaling is not fundamental for metastasis formation in this model, although it has been reported that this pathway is crucial in the trans-endothelial migration, and the subsequent metastasis formation by colon cancer cells in another orthotopic transplantation model (70).

Finally, an intriguing aspect to be clarified is whether lung metastasis express Notch ligands, like DLL4 and Jagged-1, at levels comparable to those found in the s.c. xenografts. In fact, since Notch activation in this model appears to be regulated by the ligands rather than by cell autonomous mechanisms (79,98), their levels of expression in the tumor microenvironment could be fundamental to dictate activity of the pathway in various organs.

6. REFERENCES

1. Siegel, R., Ward, E., Brawley, O., and Jemal, A. (2011) *CA Cancer J Clin* 61, 212-236
2. Cappell, M. S. (2008) *Gastroenterol Clin North Am* 37, 1-24, v
3. Fearon, E. R. (2011) *Annu Rev Pathol* 6, 479-507
4. Lynch, H. T., Shaw, M. W., Magnuson, C. W., Larsen, A. L., and Krush, A. J. (1966) *Arch Intern Med* 117, 206-212
5. Fearnhead, N. S., Wilding, J. L., and Bodmer, W. F. (2002) *Br Med Bull* 64, 27-43
6. Lynch, H. T., and de la Chapelle, A. (2003) *N Engl J Med* 348, 919-932
7. Galiatsatos, P., and Foulkes, W. D. (2006) *Am J Gastroenterol* 101, 385-398
8. Fearon, E. R., and Vogelstein, B. (1990) *Cell* 61, 759-767
9. Wharton, K. A., Johansen, K. M., Xu, T., and Artavanis-Tsakonas, S. (1985) *Cell* 43, 567-581
10. Chiba, S. (2006) *Stem Cells* 24, 2437-2447
11. Fiuza, U. M., and Arias, A. M. (2007) *J Endocrinol* 194, 459-474
12. Thurston, G., Noguera-Troise, I., and Yancopoulos, G. D. (2007) *Nat Rev Cancer* 7, 327-331
13. D'Souza, B., Miyamoto, A., and Weinmaster, G. (2008) *Oncogene* 27, 5148-5167
14. Kopan, R. (2002) *J Cell Sci* 115, 1095-1097
15. Wu, L., and Griffin, J. D. (2004) *Semin Cancer Biol* 14, 348-356
16. Iso, T., Kedes, L., and Hamamori, Y. (2003) *J Cell Physiol* 194, 237-255
17. Salat, D., Liefke, R., Wiedenmann, J., Borggrefe, T., and Oswald, F. (2008) *Mol Cell Biol* 28, 3502-3512
18. Graux, C., Cools, J., Michaux, L., Vandenberghe, P., and Hagemeijer, A. (2006) *Leukemia* 20, 1496-1510
19. Hebert, J., Cayuela, J. M., Berkeley, J., and Sigaux, F. (1994) *Blood* 84, 4038-4044

20. Weng, A. P., Ferrando, A. A., Lee, W., Morris, J. P. t., Silverman, L. B., Sanchez-Irizarry, C., Blacklow, S. C., Look, A. T., and Aster, J. C. (2004) *Science* 306, 269-271
21. Beverly, L. J., Felsher, D. W., and Capobianco, A. J. (2005) *Cancer Res* 65, 7159-7168
22. Mungamuri, S. K., Yang, X., Thor, A. D., and Somasundaram, K. (2006) *Cancer Res* 66, 4715-4724
23. Aifantis, I., Vilimas, T., and Buonamici, S. (2007) *Cell Cycle* 6, 403-406
24. Liu, W. H., Hsiao, H. W., Tsou, W. I., and Lai, M. Z. (2007) *EMBO J* 26, 1660-1669
25. Masiero, M., Minuzzo, S., Pusceddu, I., Moserle, L., Persano, L., Agnusdei, V., Tosello, V., Basso, G., Amadori, A., and Indraccolo, S. (2011) *Leukemia* 25, 588-598
26. Booth, C., and Potten, C. S. (2000) *J Clin Invest* 105, 1493-1499
27. Marshman, E., Booth, C., and Potten, C. S. (2002) *Bioessays* 24, 91-98
28. Barker, N., van de Wetering, M., and Clevers, H. (2008) *Genes Dev* 22, 1856-1864
29. van der Flier, L. G., and Clevers, H. (2009) *Annu Rev Physiol* 71, 241-260
30. Nakamura, M., Okano, H., Blendy, J. A., and Montell, C. (1994) *Neuron* 13, 67-81
31. Okabe, M., Sawamoto, K., Imai, T., Sakakibara, S., Yoshikawa, S., and Okano, H. (1997) *Dev Neurosci* 19, 9-16
32. Potten, C. S., Booth, C., Tudor, G. L., Booth, D., Brady, G., Hurley, P., Ashton, G., Clarke, R., Sakakibara, S., and Okano, H. (2003) *Differentiation* 71, 28-41
33. Nishimura, S., Wakabayashi, N., Toyoda, K., Kashima, K., and Mitsufuji, S. (2003) *Dig Dis Sci* 48, 1523-1529
34. Berdnik, D., Torok, T., Gonzalez-Gaitan, M., and Knoblich, J. A. (2002) *Dev Cell* 3, 221-231
35. Miyamoto, S., and Rosenberg, D. W. (2011) *Cancer Sci* 102, 1938-1942
36. Sander, G. R., and Powell, B. C. (2004) *J Histochem Cytochem* 52, 509-516

37. van Es, J. H., van Gijn, M. E., Riccio, O., van den Born, M., Vooijs, M., Begthel, H., Cozijnsen, M., Robine, S., Winton, D. J., Radtke, F., and Clevers, H. (2005) *Nature* 435, 959-963
38. Fre, S., Huyghe, M., Mourikis, P., Robine, S., Louvard, D., and Artavanis-Tsakonas, S. (2005) *Nature* 435, 964-968
39. Riccio, O., van Gijn, M. E., Bezdek, A. C., Pellegrinet, L., van Es, J. H., Zimber-Strobl, U., Strobl, L. J., Honjo, T., Clevers, H., and Radtke, F. (2008) *EMBO Rep* 9, 377-383
40. Jensen, J., Pedersen, E. E., Galante, P., Hald, J., Heller, R. S., Ishibashi, M., Kageyama, R., Guillemot, F., Serup, P., and Madsen, O. D. (2000) *Nat Genet* 24, 36-44
41. Suzuki, K., Fukui, H., Kayahara, T., Sawada, M., Seno, H., Hiai, H., Kageyama, R., Okano, H., and Chiba, T. (2005) *Biochem Biophys Res Commun* 328, 348-352
42. Jenny, M., Uhl, C., Roche, C., Duluc, I., Guillermin, V., Guillemot, F., Jensen, J., Kedinger, M., and Gradwohl, G. (2002) *EMBO J* 21, 6338-6347
43. Ng, A. Y., Waring, P., Ristevski, S., Wang, C., Wilson, T., Pritchard, M., Hertzog, P., and Kola, I. (2002) *Gastroenterology* 122, 1455-1466
44. Fan, X., Mikolaenko, I., Elhassan, I., Ni, X., Wang, Y., Ball, D., Brat, D. J., Perry, A., and Eberhart, C. G. (2004) *Cancer Res* 64, 7787-7793
45. Dang, T. P., Gazdar, A. F., Virmani, A. K., Sepetavec, T., Hande, K. R., Minna, J. D., Roberts, J. R., and Carbone, D. P. (2000) *J Natl Cancer Inst* 92, 1355-1357
46. Park, J. T., Li, M., Nakayama, K., Mao, T. L., Davidson, B., Zhang, Z., Kurman, R. J., Eberhart, C. G., Shih Ie, M., and Wang, T. L. (2006) *Cancer Res* 66, 6312-6318
47. Reedijk, M., Odorcic, S., Chang, L., Zhang, H., Miller, N., McCready, D. R., Lockwood, G., and Egan, S. E. (2005) *Cancer Res* 65, 8530-8537
48. Pece, S., Serresi, M., Santolini, E., Capra, M., Hulleman, E., Galimberti, V., Zurrida, S., Maisonneuve, P., Viale, G., and Di Fiore, P. P. (2004) *J Cell Biol* 167, 215-221
49. Ghaleb, A. M., Aggarwal, G., Bialkowska, A. B., Nandan, M. O., and Yang, V. W. (2008) *Mol Cancer Res* 6, 1920-1927

50. Rodilla, V., Villanueva, A., Obrador-Hevia, A., Robert-Moreno, A., Fernandez-Majada, V., Grilli, A., Lopez-Bigas, N., Bellora, N., Alba, M. M., Torres, F., Dunach, M., Sanjuan, X., Gonzalez, S., Gridley, T., Capella, G., Bigas, A., and Espinosa, L. (2009) *Proc Natl Acad Sci U S A* 106, 6315-6320
51. Fre, S., Pallavi, S. K., Huyghe, M., Lae, M., Janssen, K. P., Robine, S., Artavanis-Tsakonas, S., and Louvard, D. (2009) *Proc Natl Acad Sci U S A* 106, 6309-6314
52. Reedijk, M., Odorcic, S., Zhang, H., Chetty, R., Tennert, C., Dickson, B. C., Lockwood, G., Gallinger, S., and Egan, S. E. (2008) *Int J Oncol* 33, 1223-1229
53. Hellstrom, M., Phng, L. K., Hofmann, J. J., Wallgard, E., Coultas, L., Lindblom, P., Alva, J., Nilsson, A. K., Karlsson, L., Gaiano, N., Yoon, K., Rossant, J., Iruela-Arispe, M. L., Kalen, M., Gerhardt, H., and Betsholtz, C. (2007) *Nature* 445, 776-780
54. Noguera-Troise, I., Daly, C., Papadopoulos, N. J., Coetzee, S., Boland, P., Gale, N. W., Lin, H. C., Yancopoulos, G. D., and Thurston, G. (2006) *Nature* 444, 1032-1037
55. Sainson, R. C., Aoto, J., Nakatsu, M. N., Holderfield, M., Conn, E., Koller, E., and Hughes, C. C. (2005) *FASEB J* 19, 1027-1029
56. Li, J. L., Sainson, R. C., Shi, W., Leek, R., Harrington, L. S., Preusser, M., Biswas, S., Turley, H., Heikamp, E., Hainfellner, J. A., and Harris, A. L. (2007) *Cancer Res* 67, 11244-11253
57. Phng, L. K., and Gerhardt, H. (2009) *Dev Cell* 16, 196-208
58. Lobov, I. B., Renard, R. A., Papadopoulos, N., Gale, N. W., Thurston, G., Yancopoulos, G. D., and Wiegand, S. J. (2007) *Proc Natl Acad Sci U S A* 104, 3219-3224
59. Suchting, S., Freitas, C., le Noble, F., Benedito, R., Breant, C., Duarte, A., and Eichmann, A. (2007) *Proc Natl Acad Sci U S A* 104, 3225-3230
60. Valastyan, S., and Weinberg, R. A. (2011) *Cell* 147, 275-292
61. Fidler, I. J. (2003) *Nat Rev Cancer* 3, 453-458
62. Chambers, A. F., Groom, A. C., and MacDonald, I. C. (2002) *Nat Rev Cancer* 2, 563-572

63. Bissell, M. J., and Hines, W. C. (2011) *Nat Med* 17, 320-329
64. Thiery, J. P., Acloque, H., Huang, R. Y., and Nieto, M. A. (2009) *Cell* 139, 871-890
65. Kessenbrock, K., Plaks, V., and Werb, Z. (2010) *Cell* 141, 52-67
66. Dirat, B., Bochet, L., Dabek, M., Daviaud, D., Dauvillier, S., Majed, B., Wang, Y. Y., Meulle, A., Salles, B., Le Gonidec, S., Garrido, I., Escourrou, G., Valet, P., and Muller, C. (2011) *Cancer Res* 71, 2455-2465
67. DeNardo, D. G., Barreto, J. B., Andreu, P., Vasquez, L., Tawfik, D., Kolhatkar, N., and Coussens, L. M. (2009) *Cancer Cell* 16, 91-102
68. Gocheva, V., Wang, H. W., Gadea, B. B., Shree, T., Hunter, K. E., Garfall, A. L., Berman, T., and Joyce, J. A. (2010) *Genes Dev* 24, 241-255
69. Gupta, G. P., and Massague, J. (2006) *Cell* 127, 679-695
70. Sonoshita, M., Aoki, M., Fuwa, H., Aoki, K., Hosogi, H., Sakai, Y., Hashida, H., Takabayashi, A., Sasaki, M., Robine, S., Itoh, K., Yoshioka, K., Kakizaki, F., Kitamura, T., Oshima, M., and Taketo, M. M. (2011) *Cancer Cell* 19, 125-137
71. Carmeliet, P., and Jain, R. K. (2011) *Nat Rev Drug Discov* 10, 417-427
72. Guo, W., and Giancotti, F. G. (2004) *Nat Rev Mol Cell Biol* 5, 816-826
73. Joyce, J. A., and Pollard, J. W. (2009) *Nat Rev Cancer* 9, 239-252
74. Auguste, P., Fallavollita, L., Wang, N., Burnier, J., Bikfalvi, A., and Brodt, P. (2007) *Am J Pathol* 170, 1781-1792
75. Wyckoff, J. B., Wang, Y., Lin, E. Y., Li, J. F., Goswami, S., Stanley, E. R., Segall, J. E., Pollard, J. W., and Condeelis, J. (2007) *Cancer Res* 67, 2649-2656
76. Qian, B. Z., and Pollard, J. W. (2010) *Cell* 141, 39-51
77. Folkman, J., and Kalluri, R. (2004) *Nature* 427, 787
78. Aguirre-Ghiso, J. A. (2007) *Nat Rev Cancer* 7, 834-846
79. Indraccolo, S., Minuzzo, S., Masiero, M., Pusceddu, I., Persano, L., Moserle, L., Reboldi, A., Favaro, E., Mecarozzi, M., Di Mario, G., Screpanti, I., Ponzoni, M., Doglioni, C., and Amadori, A. (2009) *Cancer Res* 69, 1314-1323
80. Hurwitz, H., Fehrenbacher, L., Novotny, W., Cartwright, T., Hainsworth, J., Heim, W., Berlin, J., Baron, A., Griffing, S., Holmgren, E., Ferrara, N., Fyfe,

G., Rogers, B., Ross, R., and Kabbinavar, F. (2004) *N Engl J Med* 350, 2335-2342

81. Cunningham, D., Humblet, Y., Siena, S., Khayat, D., Bleiberg, H., Santoro, A., Bets, D., Mueser, M., Harstrick, A., Verslype, C., Chau, I., and Van Cutsem, E. (2004) *N Engl J Med* 351, 337-345
82. Douillard, J. Y., Siena, S., Cassidy, J., Tabernero, J., Burkes, R., Barugel, M., Humblet, Y., Bodoky, G., Cunningham, D., Jassem, J., Rivera, F., Kocakova, I., Ruff, P., Blasinska-Morawiec, M., Smakal, M., Canon, J. L., Rother, M., Oliner, K. S., Wolf, M., and Gansert, J. (2010) *J Clin Oncol* 28, 4697-4705
83. Peeters, M., Price, T. J., Cervantes, A., Sobrero, A. F., Ducreux, M., Hotko, Y., Andre, T., Chan, E., Lordick, F., Punt, C. J., Strickland, A. H., Wilson, G., Ciuleanu, T. E., Roman, L., Van Cutsem, E., Tzekova, V., Collins, S., Oliner, K. S., Rong, A., and Gansert, J. (2010) *J Clin Oncol* 28, 4706-4713
84. Amado, R. G., Wolf, M., Peeters, M., Van Cutsem, E., Siena, S., Freeman, D. J., Juan, T., Sikorski, R., Suggs, S., Radinsky, R., Patterson, S. D., and Chang, D. D. (2008) *J Clin Oncol* 26, 1626-1634
85. Saltz, L. B., Clarke, S., Diaz-Rubio, E., Scheithauer, W., Figer, A., Wong, R., Koski, S., Lichinitser, M., Yang, T. S., Rivera, F., Couture, F., Sirzen, F., and Cassidy, J. (2008) *J Clin Oncol* 26, 2013-2019
86. Dalerba, P., Guiducci, C., Poliani, P. L., Cifola, I., Parenza, M., Frattini, M., Gallino, G., Carnevali, I., Di Giulio, I., Andreola, S., Lombardo, C., Rivoltini, L., Schweighoffer, T., Belli, F., Colombo, M. P., Parmiani, G., and Castelli, C. (2005) *Cancer Res* 65, 2321-2329
87. Croner, R. S., Guenther, K., Foertsch, T., Siebenhaar, R., Brueckl, W. M., Stremmel, C., Hlubek, F., Hohenberger, W., and Reingruber, B. (2004) *J Lab Clin Med* 143, 344-351
88. Croner, R. S., Fortsch, T., Bruckl, W. M., Rodel, F., Rodel, C., Papadopoulos, T., Brabletz, T., Kirchner, T., Sachs, M., Behrens, J., Klein-Hitpass, L., Sturzl, M., Hohenberger, W., and Lausen, B. (2008) *Ann Surg* 247, 803-810

89. Joutel, A., Andreux, F., Gaulis, S., Domenga, V., Cecillon, M., Battail, N., Piga, N., Chapon, F., Godfrain, C., and Tournier-Lasserve, E. (2000) *J Clin Invest* 105, 597-605
90. Chadwick, N., Zeef, L., Portillo, V., Fennessy, C., Warrander, F., Hoyle, S., and Buckle, A. M. (2009) *Mol Cancer* 8, 35
91. Keyaerts, M., Verschueren, J., Bos, T. J., Tchouate-Gainkam, L. O., Peleman, C., Breckpot, K., Vanhove, C., Caveliers, V., Bossuyt, A., and Lahoutte, T. (2008) *Eur J Nucl Med Mol Imaging* 35, 999-1007
92. Jubb, A. M., Turley, H., Moeller, H. C., Steers, G., Han, C., Li, J. L., Leek, R., Tan, E. Y., Singh, B., Mortensen, N. J., Noguera-Troise, I., Pezzella, F., Gatter, K. C., Thurston, G., Fox, S. B., and Harris, A. L. (2009) *Br J Cancer* 101, 1749-1757
93. Patel, N. S., Li, J. L., Generali, D., Poulsom, R., Cranston, D. W., and Harris, A. L. (2005) *Cancer Res* 65, 8690-8697
94. Qiao, L., and Wong, B. C. (2009) *Carcinogenesis* 30, 1979-1986
95. Wu, Y., Cain-Hom, C., Choy, L., Hagenbeek, T. J., de Leon, G. P., Chen, Y., Finkle, D., Venook, R., Wu, X., Ridgway, J., Schahin-Reed, D., Dow, G. J., Shelton, A., Stawicki, S., Watts, R. J., Zhang, J., Choy, R., Howard, P., Kadyk, L., Yan, M., Zha, J., Callahan, C. A., Hymowitz, S. G., and Siebel, C. W. (2010) *Nature* 464, 1052-1057
96. Yamaguchi, N., Oyama, T., Ito, E., Satoh, H., Azuma, S., Hayashi, M., Shimizu, K., Honma, R., Yanagisawa, Y., Nishikawa, A., Kawamura, M., Imai, J., Ohwada, S., Tatsuta, K., Inoue, J., Semba, K., and Watanabe, S. (2008) *Cancer Res* 68, 1881-1888
97. Haruki, N., Kawaguchi, K. S., Eichenberger, S., Massion, P. P., Olson, S., Gonzalez, A., Carbone, D. P., and Dang, T. P. (2005) *Cancer Res* 65, 3555-3561
98. Serafin, V., Persano, L., Moserle, L., Esposito, G., Ghisi, M., Curtarello, M., Bonanno, L., Masiero, M., Ribatti, D., Sturzl, M., Naschberger, E., Croner, R. S., Jubb, A. M., Harris, A. L., Koeppen, H., Amadori, A., and Indraccolo, S. (2011) *J Pathol* 224, 448-460

Pubblications:

1. **Serafin, V**., Persano, L., Moserle, L., Esposito, G., Ghisi, M., Curtarello, M., Bonanno, L., Masiero, M., Ribatti, D., Sturzl, M., Naschberger, E., Croner, R. S., Jubb, A. M., Harris, A. L., Koeppen, H., Amadori, A., and Indraccolo, S. (2011) *J Pathol* 224, 448-460
2. M. Ghisi, A. Corradin, K. Basso, C. Frasson, **V. Serafin,** S. Mukherjee, Mussolin L., Ruggero K., Bonanno L., A. Guffanti, Gerosa, G. Stellin, D.M.G. D'Agostino, G. Basso, V. Bronte, S. Indraccolo, A. Amadori and P. Zanovello. "Modulation of microRNA expression in human T-cell development: targeting of Notch3 by miR-150" Blood (2011).
3. Rapp UR, Korn C, Ceteci F, Karreman C, Luetkenhaus K, **Serafin V**, Zanucco E, Castro I, Potapenko T. (2009) "Myc Is a Metastasis Gene for Non-Small-Cell Lung Cancer" PLoS ONE 4(6): e6029. doi:10.1371/journal.pone.0006029